UNIVERSITÄT SIEGEN

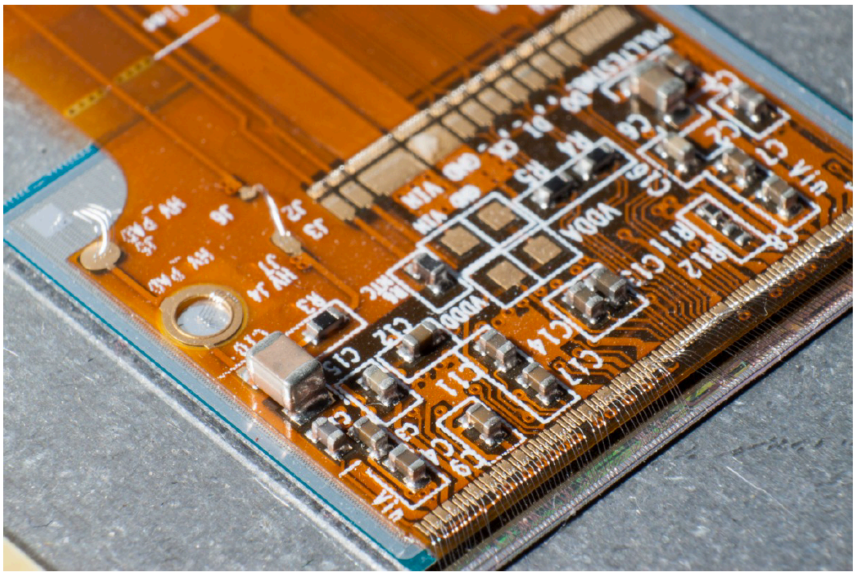

Semiconductor detectors and electronics

Master lab course

Manual v2 (12.9.2023) Beatrice Cervato

Manual v1 Niko Owtscharenko

Contact: Adam Warnerbring,
warnerbring@hep.physik.uni-siegen.de
ENC, Room EN A-203, Phone: 0271 740-3679

Responsible: Prof. Dr. Markus Cristinziani,
markus.cristinziani@uni-siegen.de
ENC, Room EN A-102, Phone: 0271 740-3926

Radiation protection: Ulrich Werthenbach,
ENC, Room EN A-001,
Phone: 0271 740-3725

Experiment Room: EN B-0111

Summary

In this two day lab course, semiconductor detectors are operated to measure ionizing radiation. First, a semiconductor diode is operated in a simple analog amplification circuit to measure single ionizing particles. Here the working principle of a diode and of the analog electronics necessary for particle detection as well as the underlying physics are introduced.
On the second day it is demonstrated how physics experiments make use of this detection principle. A state-of-the-art pixel detector from the ATLAS experiment is operated and calibrated, finally the spectrum of a radioactive source is recorded with two different techniques, comparing advantages and disadvantages.

IMPORTANT WARNING

During this experiment, you will have the great opportunity to operate a real ALTAS pixel detector module prototype as well as a separated circuit which will help you in understanding the analog chain in the detector read-out systems. This implies that you must be well prepared.

Even if you already attended electronics courses, some topics presented in the manual could be new to you. It might be obvious, but learning something new requires time and effort. Please, take this into account before choosing this (or any other) experiment.

BEFORE the day of the experiment, we expect you to:

- have the answers to ALL the “Preparation” tasks that you will find in the manual;
- have an environment for analysing the data (Excel, ROOT, Python, whatever you prefer);
- have an idea of the order of magnitude of the quantities you want to measure or set in the power supplies;
- have well understood the circuits presented in the manual.

What you will learn:

- Operation and understanding of basic analog electronics

- Understanding the working principle of detection of ionizing radiation with a semiconductor diode, especially the correlation between particle energy and signal created
- Working principle and structure of pixelated detectors for particle tracking
- Basic understanding of digitization of analog signals and of the response function of the front end electronics
- Recognizing error sources when measuring deposited charge, especially considering limited resolutions

Contents

1 Introduction

For the understanding of microscopic and macroscopic processes in physics as well as in other areas (e.g. biology, medicine) it is often important to detect ionizing particles and photons. These come for example from interactions between high-energy elementary particles or from the decay of radioactive nuclei with which biochemically active molecules are labeled. By reconstructing the tracks and the energy of these particles, it is possible to draw conclusions about the location, time and type of the underlying reaction. In modern experiments, microstructured semiconductor detectors - mostly made of silicon - are used for the highly spatially resolved detection of particle trajectories. The progressive miniaturization of manufacturing technologies and the highly integrated amplifier electronics make it possible to reconstruct a particle track down to a few micrometers.

In the first part of the experiment, the working principle of semiconductor detectors is illustrated using the example of a semiconductor diode (PIN diode) and a charge sensitive amplifier (CSA). In addition to the basics of the sensor, the essential components of the subsequent amplifier electronics are explained and their influence on the detection sensitivity of the overall system, consisting of detector and electronics, is discussed.

In the second part of the experiment, the functionality of the ATLAS front-end pixel readout chip is explained and its importance for the operation of the ATLAS detector is made clear. Furthermore, an ATLAS detector module is operated and calibrated to measure the pulse height spectrum of a γ-source.

This lab course is divided into two full days of experimentation; the semiconductor diode is part of the first day of the experiment (chapters 2 and 3), the ATLAS detector is part of the second day of the experiment (chapters 4 and 5). The basic knowledge required for the respective part of the experiment is evaluated beforehand by means of an oral examination (verbally and in writing on the blackboard) before the start of the experiment on the day of the experiment. Good preparation is a prerequisite for passing the experiment.

Knowledge and basics required for the Experiment

- Basics of electronics (for instance how to solve a circuit and calculate its gain, KVL, KCL, RC/CR circuits, ...)
- Functionality of semiconductor diodes, pn-junction
- Energy loss of charged particles in matter (Bethe-Bloch equation)
- Interaction of photons with matter (Compton effect, photoelectric effect, pair production)
- Landau distribution
- Charge sensitive amplifier (CSA)
- Pulse shaping amplifier
- Noise sources
- Equivalent noise charge (ENC)
- Position sensitive semiconductor detectors
- Structure and functionality of a pixel
- Threshold, threshold measurement (S-curve), ToT method, TDC method, charge calibration
- ^{241}Am-source

Working material

Please bring the following working material with you for the experiment:

- USB stick
- Calculator
- This script
- We also recommend bringing a laptop with python or a spreadsheet program installed to the experiment. The lab PC could be used instead.

Literature

General Information

1. W. R. Leo, **Techniques for Nuclear and Particle Physics Experiments** (!!)
   Springer Verlag
2. U. Tietze, C. Schenk, **Halbleiter-Schaltungstechnik** (!)
   Springer Verlag
3. G. Domingo, **Semiconductor Basics**
   Wiley & Sons
4. L. Rossi, P. Fischer, T. Rohe and N. Wermes, **Pixel Detectors**
   Springer Verlag
5. K. Kleinknecht, **Detektoren für Teilchenstrahlung**
   Teubner Verlag
6. S. M. Sze, **Physics of Semiconductor Devices**
   Wiley & Sons
7. P. Horrowitz, W. Hill, **The Art of Electronics**
   Cambridgde University Press
8. K. Kopitzki, **Einführung in die Festkörperphysik**
   Teubner Verlag
9. G. Lutz, **Semiconductor Radiation Detectors**
   Springer Verlag

Further Information

1. ATLAS Homepage, Technical details and photos from ATLAS,
   http://atlas.web.cern.ch/Atlas/Collaboration
2. Noise measurement:
   - P. Horrowitz, W. Hill, **The Art of Electronics**, Noise measurements and noise sources, chap. 7.18 p. 449 ff.
   - EDN Design Magazine, **Understanding and selecting rms voltmeters**,
     http://www.edn.com/design/test-and-measurement/4359579/Understanding-and-selecting-rms-voltmeters
   - EDN Design Magazine, **Calculate and measure noise values**,
     http://www.edn.com/electronics-news/4383541/Calculate-and-measure-noise-values

Part I

2

Semiconductor detectors

2.1 Energy deposition in condensed matter

When charged particles pass through matter, they can deposit energy in different ways:

- Inelastic collisions with shell electrons of matter
- Elastic collisions with atomic nuclei of matter
- Cherenkov radiation
- Bremsstrahlung
- Transition radiation
- Nuclear reactions

The mean energy loss of a charged particle passing through matter is described by the Bethe-Bloch equation:

$$-\left\langle \frac{\mathrm{d}E}{\mathrm{d}x} \right\rangle = 2\pi N_a r_e^2 m_e c^2 \rho \frac{Zz^2}{A\beta^2} \left[\ln\left(\frac{2m_e \gamma^2 v^2 W_{\max}}{I^2} \right) - 2\beta^2 - \delta - 2\frac{C}{Z} \right] \tag{2.1}$$

with:

r_e:	Classical electron radius	ρ:	Density of the absorbing material
m_e:	Electron mass	z:	Charge of the incident particle in elementary charge units e
N_a:	Avogadro constant	$\beta =$	v/c of the incident particle
I:	Mean excitation energy	$\gamma =$	$1/\sqrt{1-\beta^2}$

Z:	Atomic number of the absorber	δ :	Density correction
A:	Atomic mass of the absorber	W_{max}:	Maximum energy transfer in the event of a collision
C:	Shell correction		

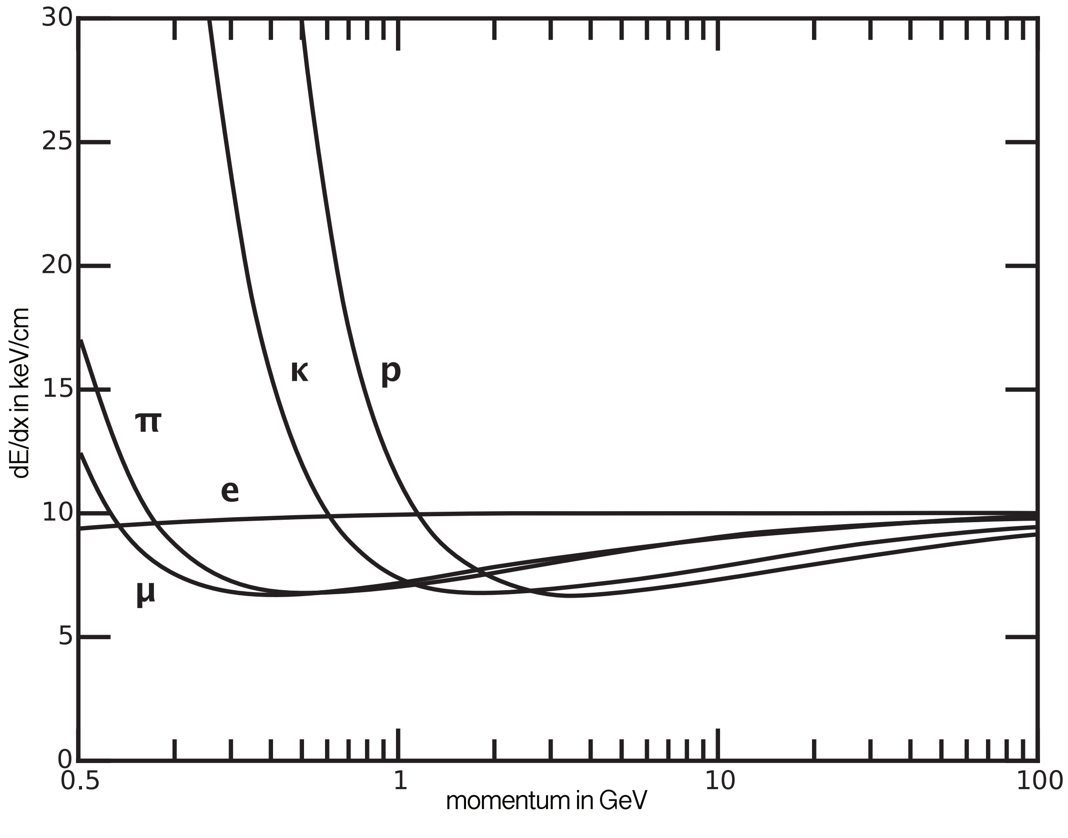

Figure 2.1: Mean energy loss of some particles in air as a function of their momentum.

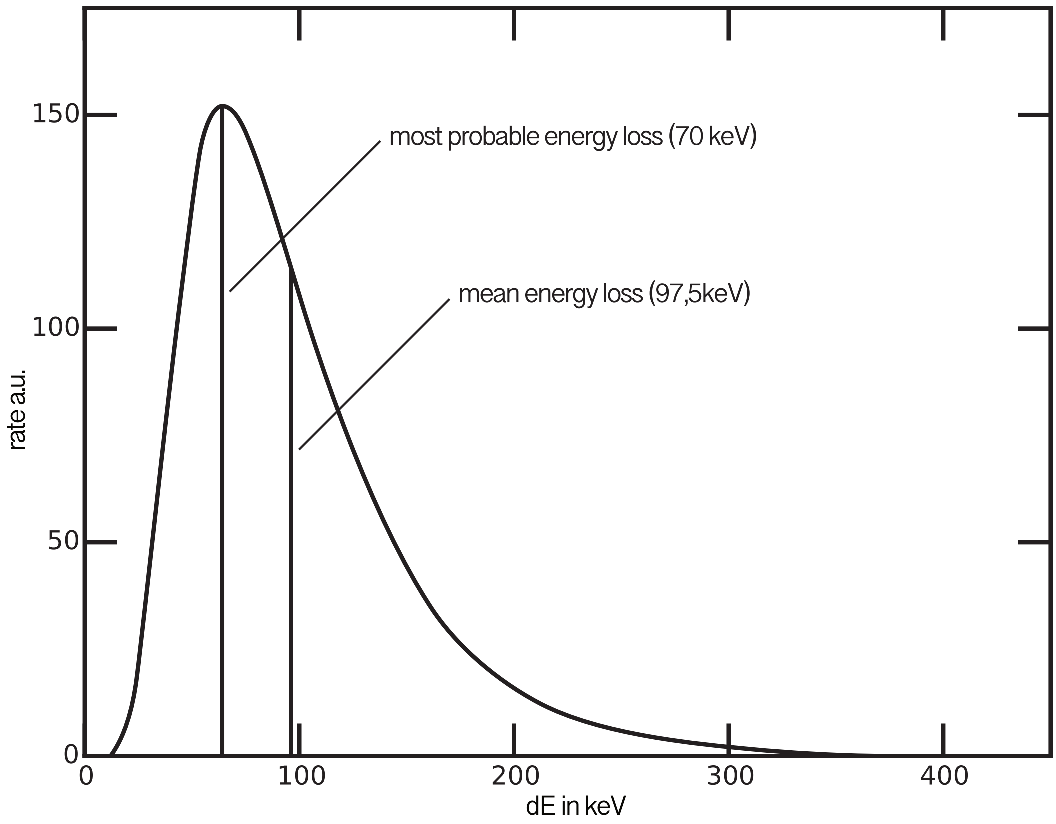

Figure 2.2: Distribution of the energy loss of a MIP in 250 µm silicon.

Since the Bethe-Bloch equation does not consider Bremsstrahlung and collisions of identical particles, it does not apply to electrons, but is a valid approximation for all heavier charged particles.

Figure 2.1 shows the average energy loss for various charged particles. The curves have a minimum at about the momentum corresponding to three times the rest mass. From there, the mean energy loss increases only slightly for higher momentum values. Particles with an energy $E > 3m_0c^2$ are called minimum ionizing particles (MIP).

For thin and medium thick detector layers the energy loss distribution corresponds to a Landau distribution (see figure 2.2). The long tail towards high energy losses dE is caused by δ-electrons (also called delta rays). A δ-electron is an electron bound in the atomic shell, which is kicked out of the atomic shell by an inelastic collision and has a comparatively large kinetic energy. The δ-electron has sufficiently large energy to ionize other atoms, causing a measurable track.

According to the central limit theorem, the shape of the Landau distribution transitions to a distribution similar to a Gaussian distribution for thick detector layers. The asymmetry of the distribution leads to different values for the most probable energy loss and the average energy loss (70 keV and 97.5 keV in 250 µm thick silicon, such as that used for the ATLAS pixel detector). The essential properties of silicon are summarized in Table 2.1.

Atomic number	14
Atomic mass	28.08 u
Dielectric constant (ϵ)	1.05 pF/cm
Band gap (E_G)	1.12 eV
Mean energy per electron-hole pair at $T = 300\,\mathrm{K}$	3.61 eV
Mobility of electrons (μ_e)	1450 cm^2/Vs
Mobility of holes (μ_h)	505 cm^2/Vs
Intrinsic charge carrier density (n_i)	$1.45 \times 10^{10}\,\mathrm{cm}^{-3}$
dE/dx of a MIP	26 keV/100 µm
Most Probable Value (MPV) for a MIP	7200 e-h pairs/100 µm

Table 2.1: Physical properties of silicon.

2.2 The semiconductor diode as a detector

Incident particles generate electron-hole pairs in a semiconductor. Describing the process in the band model, a shell electron that has been hit is lifted from the valence band into the conduction band, just like the hole is remaining in the valence band, and is therefore available as a freely moving charge carrier.
Silicon is an indirect semiconductor with a band gap $E_G = 1.12\,\mathrm{eV}$ at $T = 300\,\mathrm{K}$. For the generation of an electron-hole pair, however, 3.61 eV are required on average, since about 2/3 of the energy is lost through excitation of lattice vibrations (phonons), among other things. In 250 µm thick silicon, about 19500 electron-hole pairs are generated when a MIP is passing through (most probable value, MPV).
In order to detect the charge carriers, their recombination must be prevented. For this purpose, the electron-hole pairs are separated by an externally applied voltage. In simple silicon, however, the intrinsic conductivity is so high that the additional current generated by the incident particles would be masked. Therefore, one uses a pn junction, i.e. a diode, and operates it in reverse direction. A diode consists of an n-doped (excess of free electrons) and a p-doped layer (excess of free holes) of silicon. At the boundary layer, the free charge carriers diffuse into the other layer, recombine there and a field is created by the stationary atomic shell, which counteracts the diffusion current. Thus, a zone is formed in which there are no more free charge carriers (depletion zone).
If a reverse voltage is now applied (n-side positive compared to the p-side), this depletion zone extends (ideally) to the entire thickness of the silicon. This is referred to as a fully depleted detector.
At the electrodes, the contacts across which the voltage is applied to the diode, charge is now induced by the electrons or holes generated by the incident particles. This charge can then be processed by readout electronics.
Please make yourself familiar with the basics of a pn junction and its reverse operation in [**Domingo**].

Figure 2.3 shows the schematic structure of a typical semiconductor sensor. It consists of weakly n-doped (doping density $\sim 10^{11}\,\mathrm{cm}^{-3}$) silicon with a thin but very strongly p-doped layer (doping density $\sim 10^{19}\,\mathrm{cm}^{-3}$). This is where the pn junction is formed. On the opposite side there is still a strongly n-doped layer, which prevents the depletion zone from propagating to the electrode

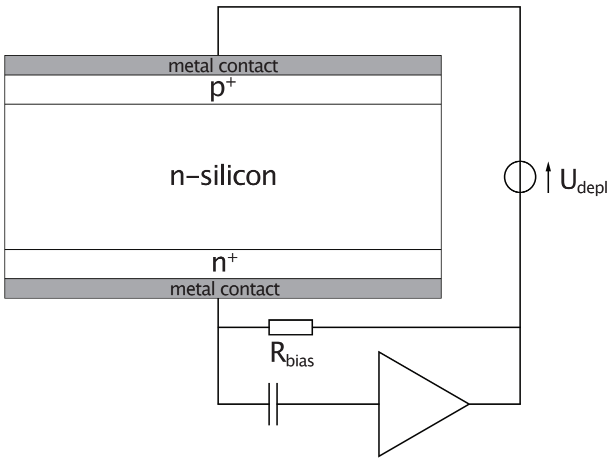

Figure 2.3: Design and operation of a semiconductor sensor.

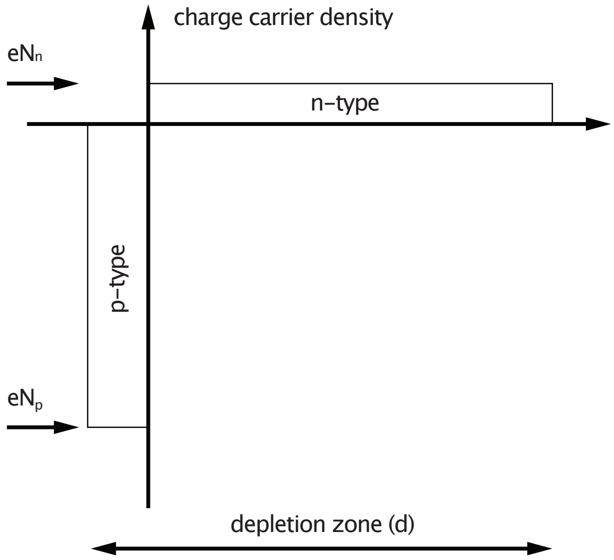

Figure 2.4: idealized space-charge distribution at a pn-junction

(metal contact). The amplifier is capacitively connected to the n-side, so electrons are collected.

2.3 Model of the pn junction

Neutrality of the total charge (charge conservation, see figure 2.4) requires:

$$N_p x_p = N_n x_n \,. \tag{2.2}$$

The electric potential and field are determined using Poisson's equation (see figure 2.5):

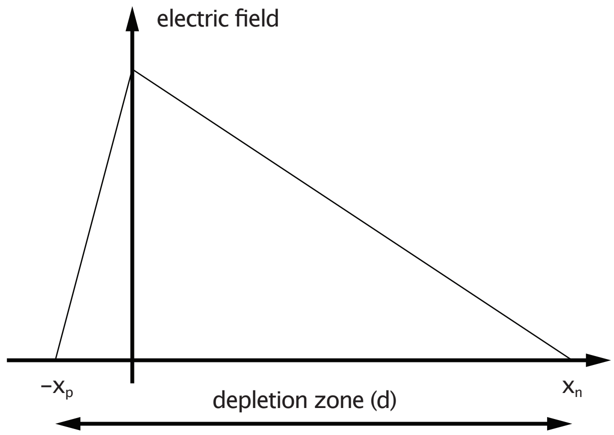

Figure 2.5: Electric field at a pn-junction

$$\frac{\mathrm{d}^2\Phi}{\mathrm{d}x^2} = -\frac{\rho(x)}{\epsilon}\,. \tag{2.3}$$

The potential difference across the junction can be obtained considering the area under the triangle (see figure 2.5):

$$U + \Phi_{\mathrm{bi}} = \Delta\Phi = E_{\max}\frac{d}{2} = eN_n\frac{d^2}{2\epsilon}\,, \tag{2.4}$$

where U is the applied voltage and Φ_{bi} is the intrinsic potential (diffusion voltage, in silicon typically about $\Phi_{\mathrm{bi}} = 0.6\,\mathrm{V}$ at $T = 300\,\mathrm{K}$). Thus, the thickness of the depletion zone increases with the square root of the applied voltage and decreases with the square root of the doping density. In addition, the pn junction behaves like a plate capacitor with plate spacing d:

$$C = \frac{\epsilon A}{d} \sim \frac{1}{\sqrt{U}}\,. \tag{2.5}$$

The detector properties are summarized in Table 2.2.

conductivity Ω of n-doped material with doping density N_n	$\Omega = 1/(e\mu_e N_n)$
Diffusion stress Φ_{bi}	$\Phi_{\mathrm{bi}} = (kT/e)(\ln(N_p/n_i) + \ln(N_n/n_i))$
(kT/e) at $T = 300\,\mathrm{K}$	$0.026\,\mathrm{V}$
Depletion depth at applied voltage V	$d = \sqrt{2\epsilon(U + \Phi_{\mathrm{bi}})/(eN_n)} = \sqrt{2\epsilon\Omega\mu(U + \Phi_{\mathrm{bi}})}$
Maximum E-field	$E_{\max} \approx eN_n d/\epsilon = 2U/d$
Capacity of the transition per unit area	$C = \epsilon/d$
Charge carrier velocity at field E	$v = \mu E$

Table 2.2: Summary of detector properties

2.4 Position reconstruction

To obtain information about the location of the passing particle, the sensitive material is divided into segments that are read out separately. The signal is generated by moving the charge carriers along the field lines toward the next electrode where they flow off.
Figure 2.6 shows some possibilities of segmentation. For example, in the strip detector, the p^+-implementation is divided into strips on one side and each strip has its own readout electronics. The holes created during particle passage are extracted to the next strip and amplified. One-dimensional location information can be obtained in this way. If the opposite side is also divided, the electrons can also be detected, and two-dimensional location information can be obtained. In the pixel detector, one side is divided into rectangles, also called pixels. Each pixel has its own readout electronics. Thus, a two-dimensional location information can be obtained without ambiguities.

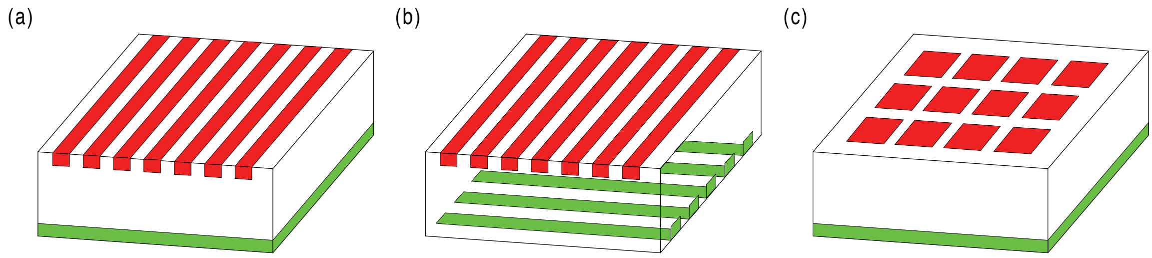

Figure 2.6: Different ways of segmentation to determine a location information: a) single side strip detector, b) double side strip detector, c) pixel detector.

2.5 Signal processing

The amplifier electronics presented in the first experimental section is typical for most semiconductor detector applications. It consists of a charge sensitive amplifier followed by a pulse shaping amplifier. Please make yourself familiar with the working principle and the golden rules of operational amplifiers (OpAmps) in [**Horowitz**, **Leo**, **TietzeSchenk**].

2.5.1 Charge sensitive amplifier

In this section, the frequency response of the charge sensitive amplifier (CSA) is discussed in detail. While this is essential for understanding the CSA working principle it is not necessary for conducting the experiment.
A charge sensitive amplifier consists of an inverting amplifier with a high gain A, which is fed back with a capacitance C_f (see Figure 2.7). Here, the amplifier input is of very high impedance, so that the input current can be neglected ("golden rules" of the operational amplifier). For the input voltage U_{in} and the output voltage U_{out} holds:

$$U_{\text{out}} = -A \cdot U_{\text{in}} \quad \text{and} \quad U_{\text{in}} - U_{\text{out}} = \frac{Q}{C_f}\,, \tag{2.6}$$

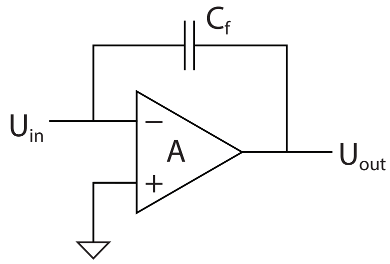

Figure 2.7: Charge sensitive amplifier.

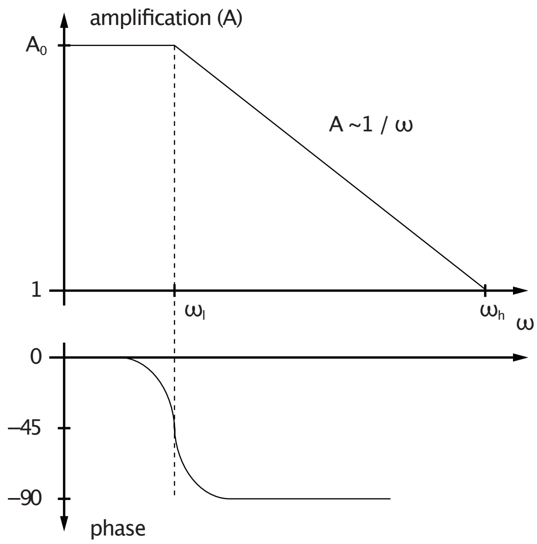

Figure 2.8: Frequency dependence of gain and phase.

where Q is the amount of charge deposited by the signal on the feedback capacitance C_f. Thus, the output voltage is

$$U_{\text{out}} = -A \cdot \frac{Q}{(A+1) \cdot C_f} \quad \text{or} \quad U_{\text{out}} = -\frac{Q}{C_f} \quad \text{for } A \gg 1. \tag{2.7}$$

In reality, the amplifier's gain A is frequency dependent (see figure 2.8). A good approximation for its frequency dependence is that of a low-pass filter

$$A(\omega) = -\frac{A_0}{1 + \frac{\omega}{\omega_l}} \,. \tag{2.8}$$

Up to the cutoff frequency ω_l the gain is

$$A = -A_0 = -\frac{\omega_h}{\omega_l} \tag{2.9}$$

and above the cutoff frequency it is

$$A = -\frac{\omega_h}{\omega} \,, \tag{2.10}$$

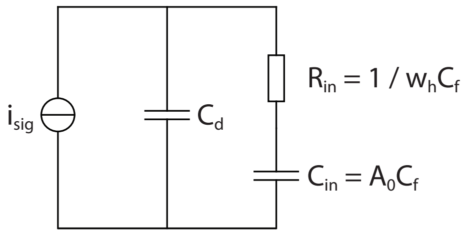

Figure 2.9: Equivalent circuit diagram for diode and charge sensitive amplifier.

where ω_h is the transit frequency at which $A = 1$. The phase shift between the inverted output signal U_{out} and the input signal U_{in} is $0°$ in the range of frequency independent gain and $-90°$ in the range of decreasing gain.
For the input signal, the charge-sensitive amplifier appears like a large capacitance in series with a resistor. The input impedance Z_{in} can be calculated as follows:

$$Z_{\text{in}} = \frac{Z_f}{A+1} \approx \frac{Z_f}{A} = -\frac{\mathbf{i}}{\omega C_f} \cdot \frac{1}{A}\,. \tag{2.11}$$

For $\omega > \omega_l$ holds:

$$A = -\mathbf{i}\frac{\omega_h}{\omega}\,, \tag{2.12}$$

Where $\mathbf{i}$ in the complex notation represents the phase shift around $90°$. Thus

$$Z_{\text{in}} = \frac{1}{\omega_h C_f} = R_{\text{in}} \tag{2.13}$$

is real and thus corresponds to an ohmic resistor.
For frequencies $\omega < \omega_l$, $A = -A_0$ and A is real (without phase shift) and thus the input impedance corresponds to

$$Z_{\text{in}} = \frac{\mathbf{i}}{\omega A_0 C_f} \tag{2.14}$$

of a capacitance with size $A_0 C_f$.

Figure 2.9 shows the equivalent circuit for a detector diode and a charge sensitive amplifier. For a small detector capacitance C_d ($A_0 C_f \gg C_d$), most of the signal charge is transferred to C_f, and the output voltage U_{out} becomes

$$U_{\text{out}} = -\frac{Q}{C_f}\,. \tag{2.15}$$

The time required for this is given by the time constant

$$\tau_{\text{in}} = R_{\text{in}} C_d = \frac{C_d}{\omega_h C_f}\,. \tag{2.16}$$

The rise time of the signal increases proportionally with the detector capacitance.
For a delta-shaped current pulse (see Figure 2.10)

$$i_{\text{sig}}(t) = Q\delta(t) \tag{2.17}$$

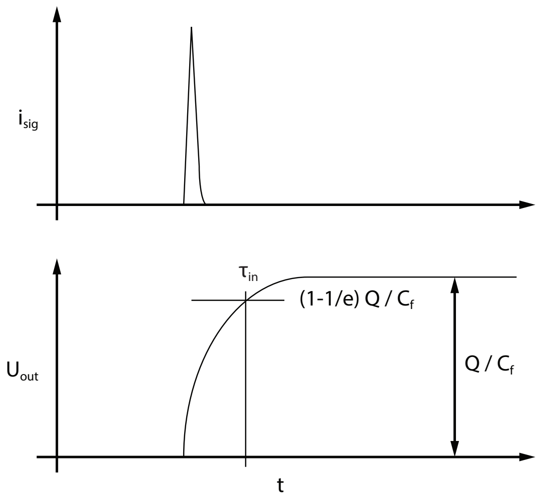

Figure 2.10: Input and output signal of the charge sensitive amplifier.

the output voltage is

$$U_{\text{out}}(t) = -\frac{Q}{C_f} \cdot \left(1 - e^{-\frac{t}{\tau_{\text{in}}}}\right) \quad \text{with} \quad \tau_{\text{in}} = \frac{C_d}{\omega_h C_f} \,. \tag{2.18}$$

In practice, a large resistor R_f is connected in parallel to the feedback capacitance C_f so that the capacitance can discharge again with a long time constant $\tau_f = R_f C_f$. Since τ_f is much larger than τ_{in}, the output signal of the amplifier can be approximated with a step function of the amplitude $\frac{Q}{C_f}$.

2.5.2 Pulse shaping amplifier

The pulse shaping amplifier changes the waveform and frequency response of the signal from the charge sensitive amplifier. In doing so, the signal is shortened, improving the time resolution of the overall system. By shortening the signal, in certain cases the pile-up, i.e. the superposition of signals that follow each other in short succession, can be prevented or reduced. Furthermore, the pulse-shaping amplifier can contribute to an improvement of the signal-to-noise ratio (S/N or SNR).

A pulse-shaping amplifier can be realized by a CR-RC filter (see Figure 2.11). In case of a step-shaped input signal, this provides a pulse of the form

$$U_S(t) = \alpha \cdot \frac{Q}{C_f} \cdot \frac{t}{\tau_S} \cdot e^{-\frac{t}{\tau_S}} \,, \tag{2.19}$$

where $\tau_S = \tau_H = \tau_T = RC$ is the time constant of high and low pass (see Figure 2.12).

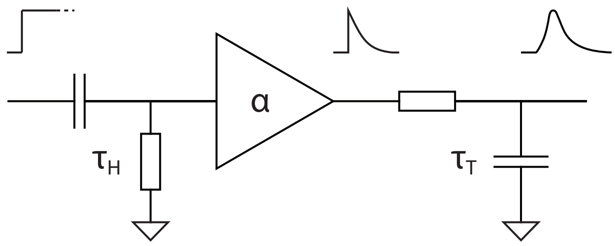

Figure 2.11: Pulse-shaping amplifier (CR-RC filter, series connection of a high-pass and a low-pass filter). The approximately step-shaped output signal of the charge-sensitive amplifier is first differentiated with the time constant τ_H to produce a short signal and then integrated with the time constant τ_T to obtain a symmetrical signal with low bandwidth.

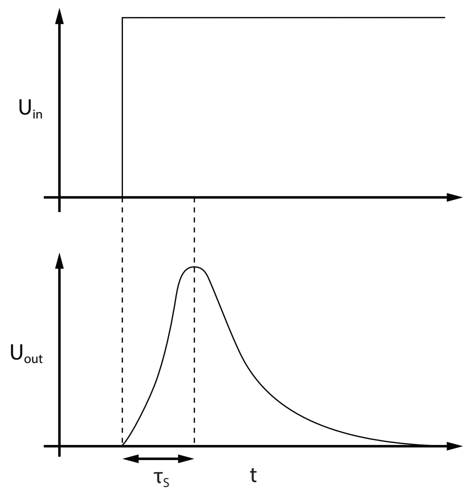

Figure 2.12: Input and output voltage in pulse forming amplifier.

2.6 Electronic noise

Noise is caused by fluctuations. A current

$$i = \frac{nev}{l} \tag{2.20}$$

passing a conductor of length l may fluctuate in the number n of charge carriers e or in the velocity v:

$$\langle i^2 \rangle = \left(\frac{ne}{l} \langle \mathrm{d}v \rangle \right)^2 + \left(\frac{ev}{l} \langle \mathrm{d}n \rangle \right)^2 . \tag{2.21}$$

There are no other physical causes for electronic noise.

2.6.1 Thermal noise

Thermal noise (also Johnson-Nyquist noise) arises from velocity fluctuations and occurs in any type of electrical conductor. The average noise voltage square $\langle v^2 \rangle$ for a conductor with resistance

R is given by

$$\langle v^2 \rangle = 4k_\mathrm{B}TR\Delta f \tag{2.22}$$

(Nyquist formula), where k_B is the Boltzmann constant and T is the temperature. The bandwidth Δf refers to the bandwidth of the measurement electronics (this includes e.g. voltmeter, amplifier and filter). The total noise is obtained by integrating over all frequencies f.
Similarly, the average noise current square $\langle i^2 \rangle$ in case of a short-circuit is

$$\langle i^2 \rangle = 4k_\mathrm{B}T\frac{1}{R}\Delta f\,. \tag{2.23}$$

The noise power spectrum in the short-circuit case (the self-generated and dissipated power for an ohmic resistor) is

$$W_\text{short circuit} = \langle v^2 \rangle / R = 4k_\mathrm{B}T\Delta f\,. \tag{2.24}$$

Thermal noise can be approximated as independent of frequency, and is also referred to as white noise in reference to optics.

2.6.2 Shot noise

Shot noise arises from fluctuations in the number of charge carriers. The current flow crossing a potential barrier (e.g. in a diode, but not in a resistor) is subject to statistical fluctuations due to the quantization of the charge. Each individual charge carrier must overcome the barrier. The average noise current square can be calculated by the equation

$$\langle i^2 \rangle = 2eI_0\Delta f \tag{2.25}$$

where e is the elementary charge, I_0 is a current, e.g. the reverse current of a detector diode, and Δf is the bandwidth of the measurement. Shot noise, like thermal noise, is frequency independent.

2.6.3 $1/f$-noise

Another type of noise, the $1/f$-noise or flicker noise, is also caused by number fluctuations and is, as the name suggests, frequency dependent. In semiconductors, charge carriers can be trapped by the lattice and released again after a lifetime τ. The superposition of many such processes with different lifetimes leads approximately to a $1/f$-distribution (more precisely: $1/f^\alpha$, where $0.5 < \alpha < 2$).
There is no unified theory about the $1/f$ noise. It also occurs in other systems, such as the rotation of the Earth, clocks, and the human voice.

2.6.4 Noise measurements

Several different approaches exist to determine noise amplitude. The most common methods [**ednmag**, **ednmag2**] use "rectify-and-average", "analog-computing"[1], thermal or "multi-sample-and-digital-computing" methods. In addition to these methods, however, it is also possible

[1] e.g. AD637 from Analog Devices

to use an analog oscilloscope or a DPO[2] to estimate the noise amplitude [**electdesgn**]. The rectify-average method was selected for this lab course. In the following, the calculation of RMS and mean is repeated. Then the rectify-average circuit used in the experiment is introduced.

Determination of RMS and mean square

For any periodic or non-periodic waveform $U(t)$, the root mean square (RMS) value in a time interval T can be calculated using the following formula:

$$U_{\mathrm{RMS}} = \sqrt{\frac{1}{T}\int_0^T U^2(t)\,\mathrm{d}t}\,. \tag{2.26}$$

In contrast, the average rectified value (ARV) results in:

$$U_{\mathrm{ARV}} = \frac{1}{T}\int_0^T |U(t)|\,\mathrm{d}t\,. \tag{2.27}$$

In general, however, the amplitude distribution $P(U)$ and not the waveform $U(t)$ is known for the electronic noise. In this case, RMS and ARV can be calculated with the following equations:

$$\begin{gathered} U_{\mathrm{RMS}} = \lim_{T\to\infty}\sqrt{\frac{1}{T}\int_{-\frac{T}{2}}^{+\frac{T}{2}} U^2(t)\,\mathrm{d}t} = \sqrt{\int_{-\infty}^{+\infty} P(U)\,U^2\,\mathrm{d}U} \\ \text{and} \\ U_{\mathrm{ARV}} = \lim_{T\to\infty}\frac{1}{T}\int_{-\frac{T}{2}}^{+\frac{T}{2}} |U(t)|\,\mathrm{d}t = \int_{-\infty}^{+\infty} P(U)\,|U|\,\mathrm{d}U\,. \end{gathered} \tag{2.28}$$

For a given waveform $U(t)$ or amplitude distribution $P(U)$, there exists a fixed relationship between U_{ARV} and U_{RMS}. Accordingly, the measurement of ARV with the knowledge of the correction factor allows the specification of the RMS value.
Below are some correction factors for calculating the ARV and RMS value from the peak voltage[3] $\hat{U}$ is given:

$$\begin{array}{lll} \text{Sine:} & U_{\mathrm{ARV}} = \frac{2}{\pi}\hat{U} & U_{\mathrm{RMS}} = \frac{1}{\sqrt{2}}\hat{U} \\ \text{Triangle:} & U_{\mathrm{ARV}} = \frac{1}{2}\hat{U} & U_{\mathrm{RMS}} = \frac{1}{\sqrt{3}}\hat{U} \\ \text{Rectangle:} & U_{\mathrm{ARV}} = \hat{U} & U_{\mathrm{RMS}} = \hat{U} \end{array} \tag{2.29}$$

Rectify-Average Circuit

The structure of the rectify-average circuit is shown in Figure 2.13. A preamplifier consisting of two inverting operational amplifiers is used to amplify the input signal. The active full-wave rectifier is a simple inverting amplifier with four diodes in the feedback loop. The diodes cause the current to always flow in the same direction through resistor R_2. For a better understanding, make yourself familiar with the current path of positive and negative input signals. The differential voltage applied to R_2 for a given input voltage U_{in} is $U_{R_2} = +\beta U_{\mathrm{in}}\frac{R_2}{R_1}$. Note that the absolute

[2]**D**igital **P**hosphor **O**scilloscope
[3]For a balanced waveform with no DC offset, $\hat{U} = \frac{1}{2}V_{\mathrm{PP}}$.

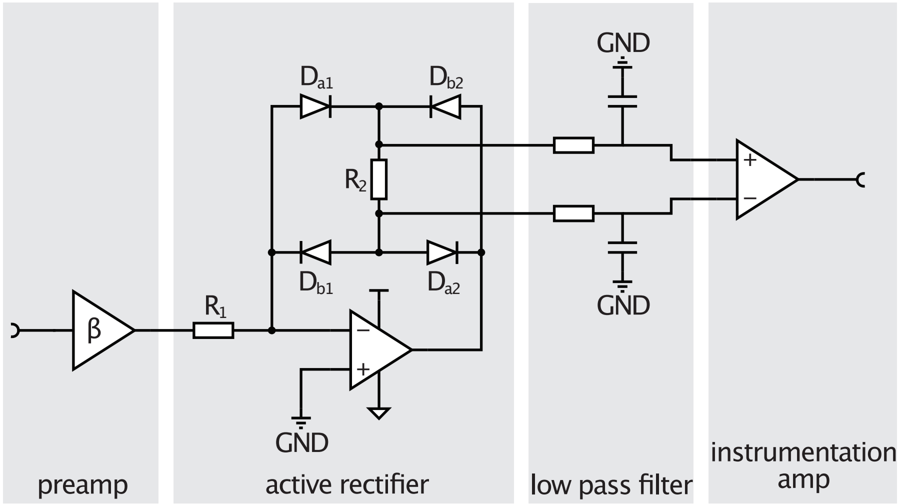

Figure 2.13: Rectify-Average Circuit.

value of the voltage across the contacts of R_2 (signal referenced to ground) varies by two times the forward voltage of the diodes, depending on the polarity of the input signal.
However, in this current-based feedback of the operational amplifier, the forward voltages of the diodes do not matter, since the differential voltage between the two terminals of R_2 is measured[4]. Schottky diodes with a low junction capacitance, fast dead time and low forward voltage were chosen for the diodes.
In principle, it is possible to realize the formation of the average value by a single RC low-pass filter after the differential voltage U_{R_2} has been determined. However, this requires an instrumentation amplifier (differential amplifier with constant gain) with very high bandwidth. To relax the requirement on the bandwidth of the amplifier, the order of difference and averaging was set according to $\langle A - B \rangle = \langle A \rangle - \langle B \rangle$ is reversed. Specifically, two simple lowpass filters ($\tau = 10\,\mathrm{ms}$) are used here for averaging and then output with the instrumentation amplifier. Incidentally, this has the advantage that the output voltages are load-independent.

2.6.5 Equivalent-Noise-Charge

The Equivalent Noise Charge (ENC) quantity denotes the noise at the output of an amplifier chain in units of the signal charge at the input:

$$\mathrm{ENC}\ [e^-] := \frac{\text{Noise at output } [V]}{\text{Signal per electron } [V/e^-]}\,, \tag{2.30}$$

or in other words, the ENC is the signal charge for which the signal-to-noise ratio (SNR) is equal to 1.
To describe the ENC mathematically, one assumes that the entire circuit is noise-free, and considers the noise sources as additional current or voltage sources connected in parallel or series with the actual signal generator (detector diode) at the input of the amplifier (see Figure 2.14).

[4]See also the data sheet of Analog Devices' AD8132, Rev. F, p. 28 for an Active Rectifier design without this advantage

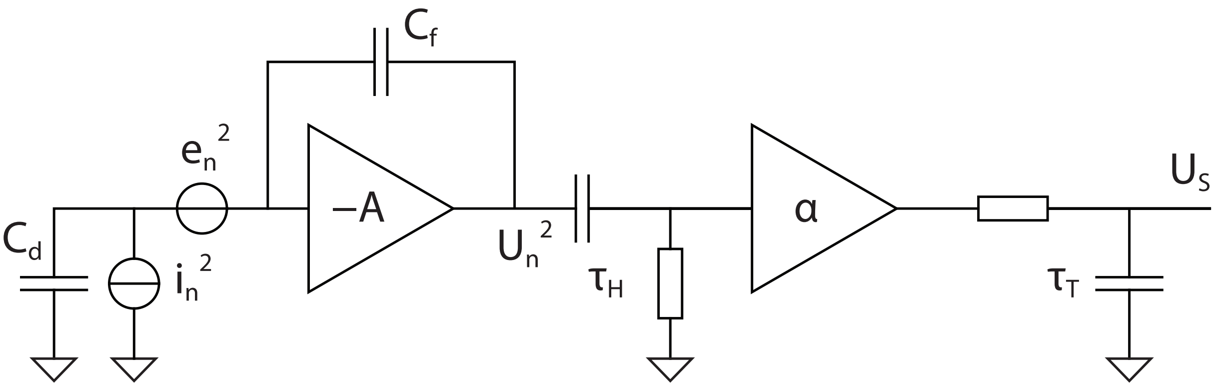

Figure 2.14: Complete system of charge sensitive and pulse shaping amplifier with noise sources.

The noise sources are characterized by the mean square noise voltage densities or noise current densities:

$$e_n^2 = \frac{\langle v^2 \rangle}{\Delta f} \quad \text{or} \quad i_n^2 = \frac{\langle i^2 \rangle}{\Delta f} \, . \tag{2.31}$$

This can be used to determine the influence of the amplifier and CR-RC filter on the noise.

Noise at the charge sensitive amplifier

The shot noise of the detector reverse current is represented by a current source i_n^2 connected in parallel to the detector diode. At the output of the amplifier, the shot noise leads to a voltage noise due to the negative feedback capacitance C_f.

$$U_{i_n}^2 = i_n^2 \cdot \left| \frac{1}{i\omega C_f} \right|^2 = 2e\langle i_{\mathrm{rev}} \rangle \frac{1}{\omega^2 C_f^2} \, , \tag{2.32}$$

which is frequency dependent. The voltage noise does not depend on the detector capacitance. Another source of noise is the input transistor of the amplifier. This point of the switching circuit is particularly relevant, because the amplification of the signal takes place at the input transistor. In the channel of a field-effect transistor thermal noise is generated, which can be described as a noise voltage source e_n^2 connected in series to the input gate:

$$\langle v_{\mathrm{therm}}^2 \rangle = 4k_{\mathrm{B}}T \frac{2}{3} \frac{1}{g_m} \Delta f \, , \tag{2.33}$$

where $g_m = \frac{\delta I_{\mathrm{drain}}}{\delta V_{\mathrm{GS}}}$ is the transconductance of the transistor.
In addition, $1/f$ noise is generated in the transistor, which also manifests itself as a serial voltage source at the input gate:

$$\langle v_{1/f}^2 \rangle = K_{1/f} \frac{1}{f^\alpha} \Delta f \, . \tag{2.34}$$

$K_{1/f}$ is a constant and depends on geometrical and material properties of the transistor.
At the output of the amplifier, thermal and $1/f$ noise result in a voltage of

$$U_{e_n}^2 = e_n^2 \cdot \left(\frac{C_d + C_f}{C_f} \right)^2 = \left(4k_{\mathrm{B}}T \frac{2}{3} \frac{1}{g_m} + \frac{K_{1/f}}{f^\alpha} \right) \cdot \left(\frac{C_d + C_f}{C_f} \right)^2 , \tag{2.35}$$

where $\frac{C_d+C_f}{C_f}$ is the voltage gain of the charge-sensitive amplifier with upstream detector capacitance C_d. The larger the detector capacitance C_d, the greater the noise.

Influence of the pulse shaping amplifier on the noise

The magnitude square of the transfer function of a CR-RC filter with $\tau_S = \tau_H = \tau_T$ is:

$$|H(\omega)|^2 = \left| \underbrace{\frac{1}{1+\frac{1}{i\omega\tau_S}}}_{\text{High pass}} \cdot \underbrace{\frac{1}{1+i\omega\tau_S}}_{\text{Low pass}} \right| = \frac{\omega^2\tau_S^2}{\omega^2\tau_S^2+1} \,. \tag{2.36}$$

The influence of the filter on the noise signal at the output of the charge-sensitive amplifier can be calculated using the carry function. The average noise voltage square $\langle U^2 \rangle$ at the output of the filter is

$$\langle U^2 \rangle = \int_0^\infty |H(\omega)|^2 \left[U_{i_n}^2 + U_{e_n}^2\right](\omega)\, \mathrm{d}\omega \,. \tag{2.37}$$

If we perform the integration and assume that i_n^2 and e_n^2 are not correlated, we obtain

$$\mathrm{ENC}^2 = \underbrace{\ldots \langle i_{\mathrm{rev}} \rangle \cdot \tau_S}_{\text{Shot noise}} + \underbrace{\ldots C_d^2/\tau_S}_{\text{thermal noise}} + \underbrace{\ldots C_d^2}_{1/f-\text{noise}} \tag{2.38}$$

and thus

$$\mathrm{ENC}^2 = a \cdot 2e\langle i_{\mathrm{rev}} \rangle \tau_S + b \cdot 4k_{\mathrm{B}}T \frac{2}{3}\frac{1}{g_m}\frac{C_d^2}{\tau_S} + c \cdot K_{1/f}\frac{1}{f^\alpha}C_d^2 \,. \tag{2.39}$$

Of the constants a, b and c, $c = 0$ is set in the following, since the $1/f$ noise is neglected in this experiment (carrier trapping is negligible in unirradiated and undamaged silicon).

3

Experiment I - Semiconductor diode and signal electronics

3.1 Experiment - Properties of a PIN diode

In this part of the experiment, the essential electrical properties of a silicon detector are illustrated using a PIN diode.
For this purpose, use circuit 1 (see Figure 3.1) and the detector diode shielded in the metal case. This setup consists of an operational amplifier (opamp) connected to the feedback resistor R_{F1} and the impedance Z_D of the detector diode as an inverting amplifier. The negative detector voltage U_D is applied to the diode via the high impedance bias resistor R_B.

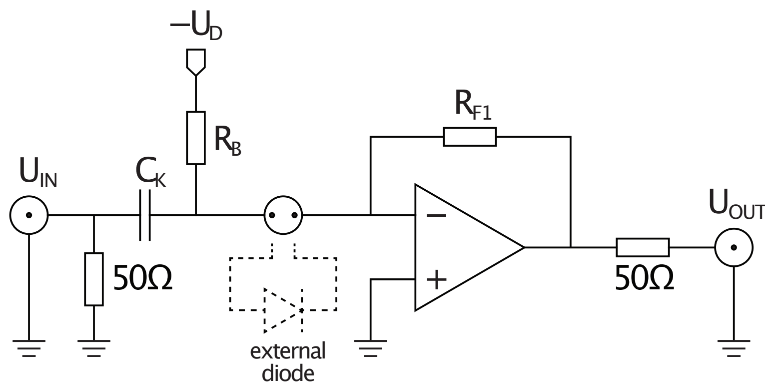

Figure 3.1: **Circuit 1** to investigate the properties of the PIN diode ($C_K = 50\,\mathrm{nF}$, $R_B = 5.1\,\mathrm{M\Omega}$, $R_{F1} = 10\,\mathrm{M\Omega}$).

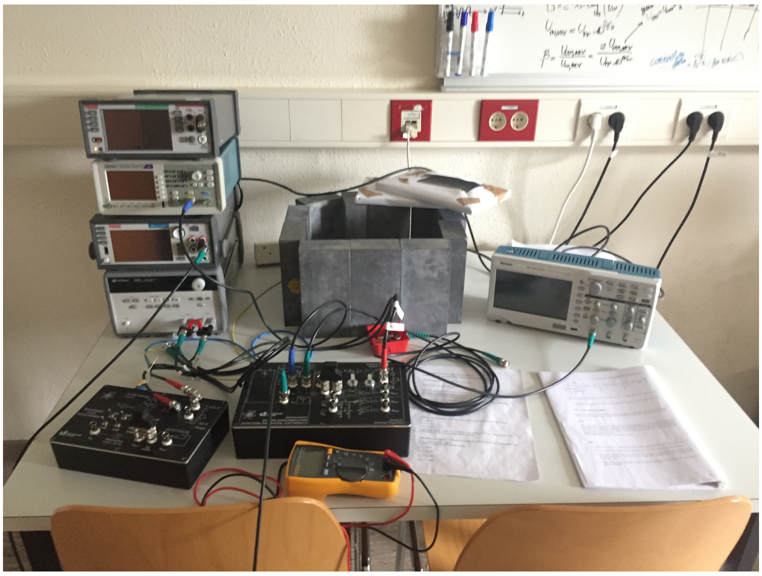

Figure 3.2: Desk equipped for the first-day experiment.

Setup

To measure the detector capacitance, an AC signal can be coupled in via the coupling capacitor C_K. To do this, connect the function generator to input U_{IN} and set a sinusoidal signal ($f = 1\,\text{kHz}$) with suitable amplitude (much smaller than the detector voltage) and measure the `RMS` voltage at U_{OUT}. To determine the leakage current, measure the DC value of the output voltage at U_{OUT} (no input signal at U_{IN}) and correct the measured values for the output offset.
Also note the properties of silicon in table 2.1 and the detector properties in table 2.2.

Practical tips

Apart from the cables and the circuits, on your desk (see Figure 3.2) you will find the following devices that must be properly set up.

- First power supply (Figure 3.3): it must be used to supply the active elements of the circuit(s). If you are not using the rectifier (smaller black box), connect it just to the unit with the diode (bigger black box).
  - Press the button `RECALL`, on the screen will appear "`STATE I`", press `RECALL` again;
  - without any cable connected, press the button `Output ON/OFF` and, using the handheld multimeter, check that the "Output 1" is at +15 V while the "Output 2" is at - 15 V;
  - switch OFF the output and proceed to connect the power supply to the first unit, using the labelled cables;
  - switch ON the output again.
- Second power supply (Figure 3.4): it must be used to deplete the diode. Keep in mind that:

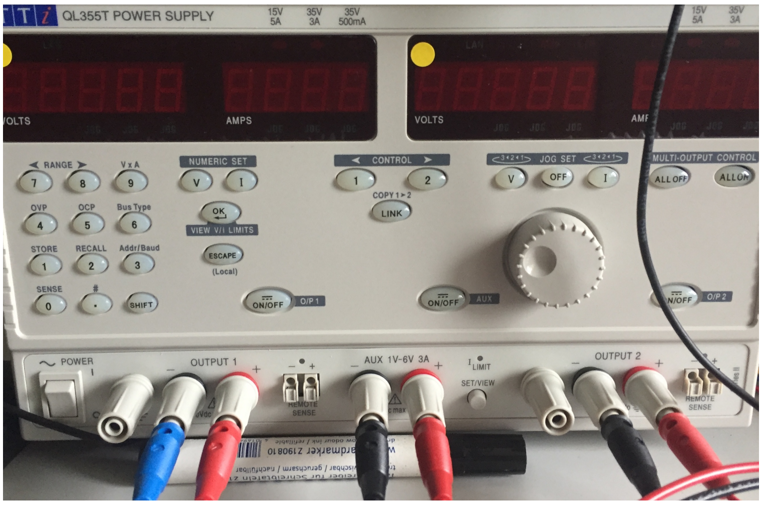

Figure 3.3: First power supply, used for the active parts of the circuits.

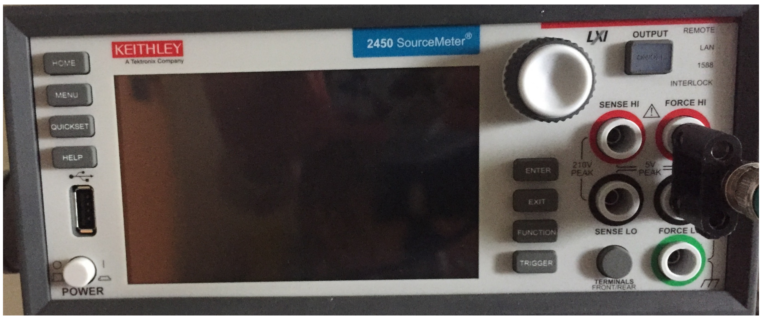

Figure 3.4: Second power supply, used for the bias voltage of the diode.

- only negative values must be used;
- the correct range must be set (by default it is 200 mV, but you usually want to have $\sim$ -40 V, thus use the 20 V or the 200 V scale);
- a green and bright "F" must be there (you are using the front output of the sourcemeter, not the rear one).

- Function generator (Figure 3.5): it is used to give a "fake" signal as input to the different electronic chains, simulating the signal produced by the diode or by the former electronics block.
- Digital multimeter (Figure 3.6): used in several tasks for voltage measurement. Keep in mind that:
  - the light near `Front` must be green;
  - the cable must be in the `INPUT` column (not in the `SENSE WIRE` one);
  - the correct measurement mode must be chosen! In particular, we will use the ACV or DCV mode. The ACV mode should be used whenever you expect to have an AC output, for example when you are measuring C_D or C_{para}. The DCV mode,

Figure 3.5: Function generator, is used for simulating the signal coming from the diode or other parts of the circuit.

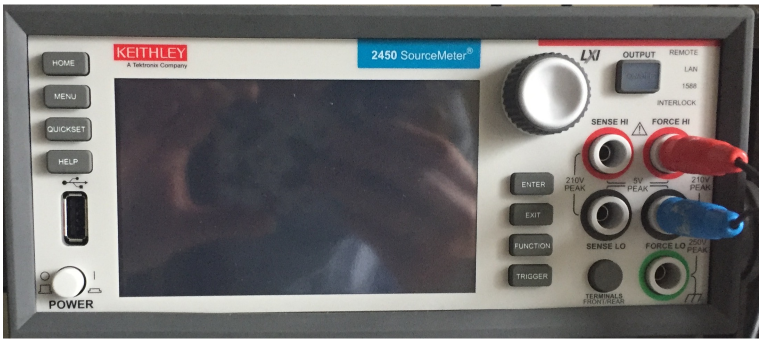

Figure 3.6: Digital multimeter.

instead, should be used whenever you expect to have a DC output, for example in the measurement of the leakage current of the detector (of course, you are measuring $U_{out,DC}$ and derive I_D afterwards).

Tasks

Preparation

1. Derive the formula for the gain of this circuit. How can you determine the detector capacitance from this, how the contribution of the leakage current?

2. Why is C_K negligible? What role does the magnitude of R_B play? Can this influence the performance of the measurement (consider time constant $C_K \cdot R_B$)?

Measurements

3. Determine the correction of the output voltage. How would you do this?
   Note: In a real operational amplifier, there exist parasitic input currents $I_{\mathrm{IN},U_\pm}$ and an

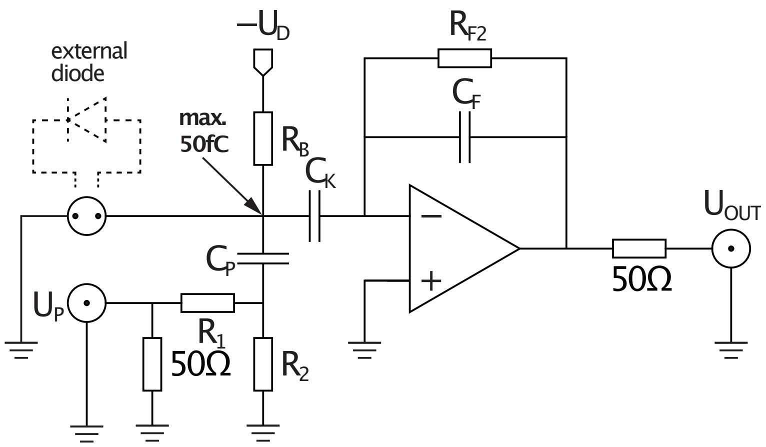

Figure 3.7: **Circuit 2**, charge sensitive amplifier with calibration input ($C_K = 10\,\mathrm{nF}$, $C_P = 1.5\,\mathrm{pF}$, $R_B = 5.1\,\mathrm{M\Omega}$, $R_{F2} = 4.1\,\mathrm{M\Omega}$, $C_F = 1\,\mathrm{pF}$, $\frac{R_2}{R_1+R_2} = \frac{1}{50}$).

input offset voltage U_{OS}, which is needed to make the output voltage 0 V. Thus, the measured value is $U_{\mathrm{OUT}} \approx \langle i_{\mathrm{rev}} \rangle R_{F1} - I_{\mathrm{IN},U_-} R_{F1} - U_{\mathrm{OS}}$.

4. Determine the parasitic capacitance of the assembly.

5. Measure the dependence of the detector capacitance C_D as well as the leakage current I_D on the detector voltage U_D **do not apply more than** $-80\,\mathrm{V}$ of detector voltage.

Analysis

6. Plot the corrected capacitance C_D against U_D appropriately (see formula 2.5) and determine the depletion voltage as well as the capacitance of the fully depleted diode.

7. Using these values, determine the thickness of the depletion zone in the diode (diode area $1\,\mathrm{cm}^2$) and the doping density N_D.

8. Calculate the electric field in the fully depleted diode. Derive the velocity of the charge carriers and estimate the charge collection time.

3.2 Experiment - Amplifier electronics

3.2.1 Charge sensitive amplifier

The charge sensitive amplifier in circuit 2 (see figure 3.7) consists of a low noise inverting amplifier fed back with a capacitor C_F and a resistor R_{F2} in parallel. The capacitance C_K isolates the input of the amplifier from the detector leakage current (DC current). Its dimension is chosen to have no influence on the detector signal ($C_K \gg C_D$). It can therefore be neglected in the following. In addition, there is another capacitance C_P at the input of the amplifier. By applying a voltage step U_P to this capacitance, a defined amount of charge can be fed to the amplifier input from outside. This calibration circuit can be used to simulate a charge signal of known magnitude and to determine the charge gain of the system

$$G = \frac{U_{\mathrm{OUT}}}{Q_{\mathrm{IN}}} \tag{3.1}$$

In order to stay within the linear input range of the charge sensitive amplifier, it is important for the input charge Q_{IN} to not exceed 50 fC during calibration.

Setup

Connect the function generator to the test input of circuit 2 (indicated by the square wave symbol below the socket) and select a suitable pulse shape. The detector diode must be connected for all subsequent measurements and is operated fully depleted, since the system is to be calibrated for the source measurement.

Tasks

Preparation

1. Consider the voltage divider behind the test input of circuit 2 and state the relationship between the amount of charge at capacitance C_P and pulse generator amplitude U_P.
2. What effect limits the maximum frequency of the test pulses and what amplitude should be chosen?

Measurements

3. Connect the output of the preamplifier to the oscilloscope and record the waveforms at different frequencies. Again SYNC or the signal itself can be used for triggering.
4. What is the gain of the system in mV/electron?
5. Using the measured gain and pulse shape, determine R_{F2} and C_F and compare the results to the actual values.

3.2.2 Pulse shaping amplifier

Figure 3.8 shows the pulse shaping amplifier consisting of a high pass and a low pass (CR-RC filter). The push buttons can be used to set 15 different time constants for the filters (0 = OFF).

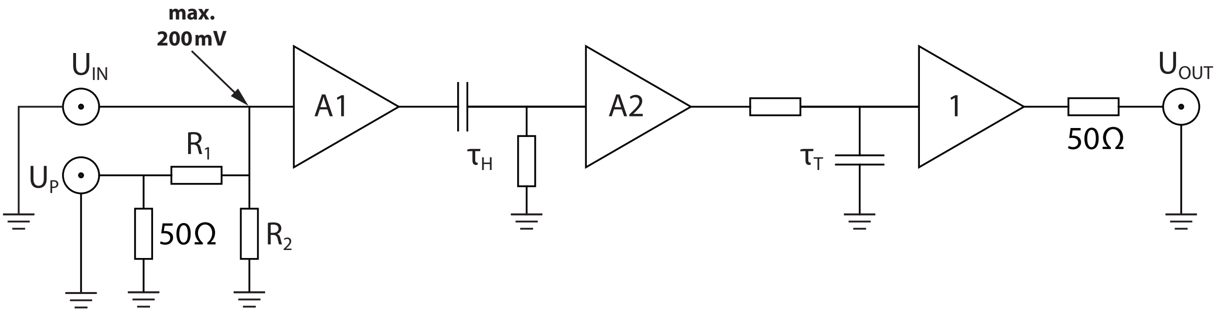

Figure 3.8: **Circuit 3**, pulse shaping amplifier (τ_H and τ_T adjustable via the push button; $R_1 = 2.5\,\mathrm{k\Omega}$ and $R_2 = 50\,\Omega$).

Setup

Now connect the square wave signal of the function generator to the test input of the pulse shaping amplifier (marked by the square wave signal symbol below the socket). To protect the pulse shaping amplifier, the amplitude at the input node of the amplifier must not exceed 200 mV. The test input of circuit 3 has a voltage divider (R_1 and R_2) for this reason, but not the socket used to connect circuit 2 and 3.
CAUTION: Make sure to use the correct socket!

Tasks

Measurements

1. View and record the output signal of the pulse shaping amplifier with the oscilloscope.

2. First switch off the high and low pass (switch to 0) and measure the voltage gain A.

3. After that, measure the time constant and the gain for all settings from 1 to F (both switches on identical values, so $\tau_H = \tau_T$). Note the definition of the time constants given in Section 2.5.2!

Analysis

4. Why and how does the signal amplitude change when the time constants for high and low pass are different?

3.2.3 Connection of charge sensitive preamplifier and pulse shaping amplifier

Setup

Now connect the output of circuit 2 to one channel of the oscilloscope and from there with a T-piece to the input of circuit 3. Also connect the output of circuit 3 to the oscilloscope. Generate calibration pulses at the test input of circuit 2. Observe and record the resulting signals at the output of the charge sensitive and pulse shaping amplifiers.

Tasks

Measurements

1. View and record the signals when varying the frequency and amplitude of the calibration signal, and the time constants τ_H and τ_T of the pulse shaping amplifier.
2. Determine the total system gain in mV/electron for all 15 switch combinations with $\tau_H = \tau_T$.

Analysis

3. Discuss the influence of the time constant.
4. What happens to the waveform when time constants τ_H and τ_T come to the order of the preamplifier time constant $(R_{F2} \cdot C_F)$? How do you explain this effect?
5. Compare this gain with the values already measured individually for the charge-sensitive and pulse-shaping amplifiers. Consider the 1:2 voltage divider consisting of the $50\,\Omega$ output resistance of circuit 2 and resistor R_2 in circuit 3.

3.2.4 Noise in signal electronics - Optional

Setup

For the electronic noise measurements, disconnect the pulse generator from the input of circuit 2 and determine the magnitude of the noise. If possible, also disconnect the oscilloscope from the circuit (Why?).

Calibration

First, the rectify-average circuit must be calibrated.

1. Measure the gain of the circuit (note: factor β, see Figure 2.13). Use the function generator and choose a suitable waveform. Pay attention to the relation between $\hat{U} \leftrightarrow U_{\mathrm{PP}}$, $U_{\mathrm{RMS}} \leftrightarrow U_{\mathrm{ARV}}$ for your chosen waveform. Furthermore, the selected signal frequency should not fall below or exceed the bandwidth of the circuit. The input of the rectify-average circuit has a $50\,\Omega$ input impedance. Make sure that the input signal does not exceed the dynamic range of the Rectify-Average circuit. Observe the output voltage of the rectify-average circuit. Use an attenuator to attenuate the signal of the pulse generator [1]. Take measurements at different attenuations.

2. The gain of the circuit is generally a function of the signal frequency, the input voltage, the offset voltage and the temperature. In the case presented here, however, these effects can be neglected.

3. Calculate the correction factor $\frac{U_{\mathrm{RMS}}}{U_{\mathrm{ARV}}}$, see formula 2.28. Assume a normally distributed noise with an amplitude distribution of $\mu = 0$:

$$P(U) = \frac{1}{\sigma\sqrt{2\pi}} \exp\left(-\frac{1}{2}\left(\frac{U-\mu}{\sigma}\right)^2\right). \tag{3.2}$$

ENC measurement

After you have determined the charge gain of the complete system, it is now possible to convert the measured noise voltages into an input charge (ENC).

Tasks

1. Vary the capacitance at the input of the charge sensitive amplifier using different capacitors. Determine the ENC values and plot them as a function of load capacitance.

2. Use the $70\,\mathrm{pF}$ capacitance or alternatively the fully depleted diode and vary the time constant τ_S of the pulse shaping amplifier. Plot the ENC values against τ_S. Note that the gain of the pulse shaping amplifier changes slightly depending on the switch position (see the previous measurements).

3. For which time constant does the noise become minimal?

Optional: Quick estimation of the noise

A quick way to estimate the noise without additional measurement electronics is to observe the signal on an oscilloscope. To do this, select a high afterglow time in the "Display" menu of the oscilloscope. In this mode of operation, each trigger event is displayed on the screen without erasing the previous signal. Use a large time scale. A wide band will now appear on the screen from which you can estimate the σ width of the Gaussian distributed noise.

[1] Rohde & Schwarz, Application Note 1MA98, https://scdn.rohde-schwarz.com/ur/pws/dl_downloads/dl_application/application_notes/1ma98/1MA98_13e_dB_or_not_dB.pdf

4. Repeat one of the series of measurements made with the Rectify-Average circuit using this method and compare the two results.

5. How many σ of a Gaussian distribution corresponds to the range you see on the oscilloscope

3.2.5 Complete system

Setup

Now connect the PIN diode from the first part of the experiment to the amplifier and fully deplete it.
Now have the assistant show you how to handle the radioactive source (^{241}Am). Put the radioactive source above the detector diode and use the lead shielding.

Tasks

1. Calculate the optimum time constant τ_S for the measured leakage current and the measured capacitance according to the formula 2.39 ($g_m = \frac{1}{200}\,\Omega^{-1}$, $a = b = 1$, $c = 0$). Does this value match the measurement from section 3.2.4?

2. At which setting of the filter is the signal-to-noise ratio the highest?

3. What kind of pulse height spectrum do you expect?

4. What energies does this correspond to (approximately)?

5. Observe and record single pulses from energy deposition of the radiation in the diode. Use the measured gain of the system to calculate the energy deposited in the diode from the pulse height.

6. What would you expect to see in a β emitter (electrons)?

Part II

4

Pixel detectors

In the second part of the experiment, the FE-I4[1] pixel readout chip with 80×336 readout channels is operated. The FE-I4 serves as a readout chip for pixel sensors. Charge generated in the sensors is measured using the FE-I4 and the readings are temporarily stored in the chip until the detector readout system digitally reads out the readings along with the location information. The FE-I4 is used for the innermost layer of the vertex and tracking detector in the ATLAS experiment. In the following chapters the ATLAS pixel detector and the FE-I4 pixel readout chip will be described in more detail.

4.1 LHC, ATLAS and the pixel detector

In 2008, the LHC[2] at CERN[3] in Geneva, planned since 1994, went into operation for the first time. After the quenching of a superconducting connection at one of the accelerator magnets and a one-year break in operation, the LHC was able to resume operation in 2009.
The LHC is a ring accelerator at which proton bunches are accelerated along a circular path in opposite directions. The proton bunches are brought to collision at a total of four interaction points. The four large-scale experiments (ATLAS, CMS, LHCb and ALICE), which focus on different physics questions, are located there.
About 10^{11} protons are bundled in each proton bunch. The collision rate at the interaction points is 40 MHz, corresponding to a time separation of 25 ns. The luminosity[4] of the accelerator is to be gradually increased from initially less than $10^{33}\,\mathrm{cm}^{-2}\mathrm{s}^{-1}$ to as high as $5 \times 10^{34}\,\mathrm{cm}^{-2}\mathrm{s}^{-1}$ in 2022.
The main goals of the ATLAS experiment, in which the Physics Department of the University of Siegen is involved, are:

[1] **F**ront-**E**nd chip, **I**BM technology, **4**. Generation

[2] **L**arge **H**adron **C**ollider

[3] **C**entre **E**uropéen pour la **R**echerche **N**ucléaire

[4] A measure of the interaction rate, the expected event rate $\dot{N}$ is calculated from the luminosity L and the effective cross section σ as follows: $\dot{N} = \sigma \cdot L$. In a ring accelerator colliding n packets at repetition frequency f and whose packets have particle number N_1 and N_2 and cross-sectional area A, $L = \frac{n \cdot N_1 \cdot N_2 \cdot f}{A}$.

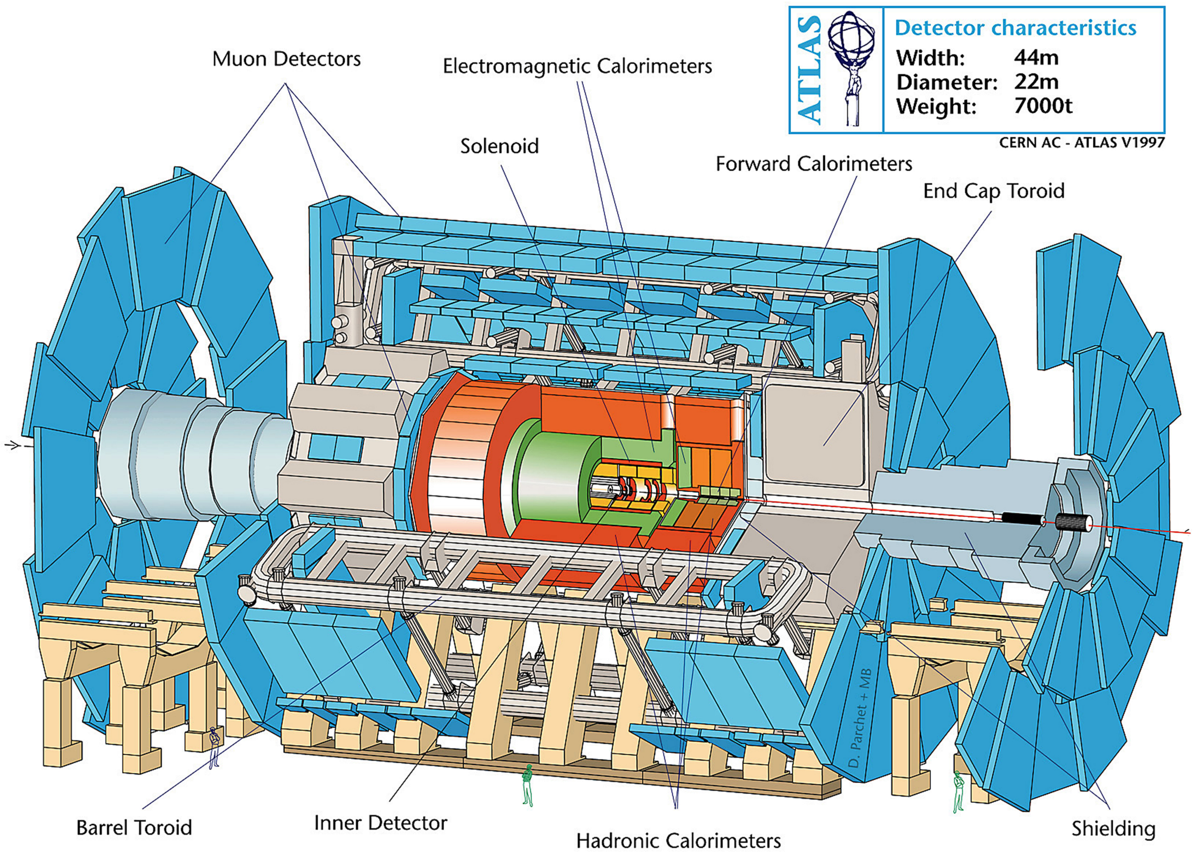

Figure 4.1: The ATLAS detector and its subsystems.

- The search for the Higgs boson predicted by the Standard Model and its detection, which succeeded in 2012 [**Aad20121**].
- In an extension of the Standard Model (minimal supersymmetric Standard Model, MSSM), there are three neutral and two charged Higgs bosons.
- The study of CP-violating decays of the B meson.
- The extension of the Standard Model, e.g. the search for supersymmetric particles.

The ATLAS detector (Figure 4.1) is 42 m long, 22 m high, and has a mass of approximately 7000 t. It is divided into several subdetector systems, which are briefly described below:

- The inner detector
  It forms the core of the ATLAS detector, it is 6.80 m long and it has a radius of 2.30 m. Its task is the precise position and momentum measurement of the individual particle trajectories. For this purpose, the pixel detector with a spatial resolution of 80–100 µm in beam direction (z) and 12–15 µm in $r\phi$ direction is located around the interaction point. This is enclosed by several layers of silicon strip detectors (SCT[5]) with a resolution of 20 µm

[5]**S**emi-**C**onductor-**T**racker

in the rϕ direction and 700 µm in the z direction. The outermost shell of the inner detector is formed by the TRT[6], which provides about 30 trace points per particle passage and is also used for energy loss measurement and electron identification.
The entire inner detector system is located in a 2 T strong solenoidal magnetic field to perform momentum measurements.

- The Calorimeter system
  The Calorimeter system consists of an electromagnetic and hadronic calorimeter for measuring the energy and direction of particles and particle jets.

- The muon spectrometer
  It forms the outer shell of the ATLAS detector and is responsible for detecting muons and measuring their momenta. The required magnetic field is generated by the toroidal magnetic field coils (about 3.9 T). Fast triggers (Level1 triggers) for event preselection are also generated from the signals of the muon spectrometer.

The ATLAS Pixel Detector: Modules, Staves, Barrels and End Caps

The pixel detector is part of the vertex and tracking detector. The pixel detector consists of readout chips, sensors and a holding structure. It is about 1.3 m long, has a diameter of 35 cm and a mass of about 4.4 kg.
Since parallel readout of all pixels of the readout chip is desired, the difficulty is that each readout channel requires its own readout electronics (preamplifier, signal processing) and these cannot be accommodated at the edge of the sensor, as is the case, for example, with strip detectors or CCDs[7]. The sensor and readout electronics are processed on different wafers and connected together using a special technique so that readout channels are available over the entire area. Due to the separation of sensitive material (sensor) and readout electronics (readout chip), this is referred to as a hybrid pixel detector.
Readout chips and sensors are connected to each other using the flip-chip process. In the flip-chip process, solder bumps are applied to all pixels of the readout chip on the bond pads provided for this purpose. After the two contact surfaces of the readout chip and sensor have been placed on each other, the melting and subsequent solidification of the solder creates an electrically conductive and permanent mechanical connection between the sensor and the readout electronics (see Figure 4.2).
Just like the readout chips, the sensors are divided into segments (sensor pixels), each of which is connected to a pixel of the readout chip. This makes it possible to obtain two-dimensional position information. The doping of the front side of the silicon sensors (n^+-side) is divided, whereas the back side (p^+-side) is homogeneously doped. The negative high voltage is applied to the sensor backside, which enables the collection of electrons by the amplifier electronics of the readout chip.

The smallest functional unit of a hybrid pixel detector is called a module. The modules are glued to elongated carbon fiber structures called staves. The staves contain the cooling tubes as well as interconnection of power supply and data transmission. Several staves are then arranged parallel

[6] **T**ransition-**R**adiation-**T**racker (transition radiation detector)
[7] **C**harge **C**oupled **D**evice

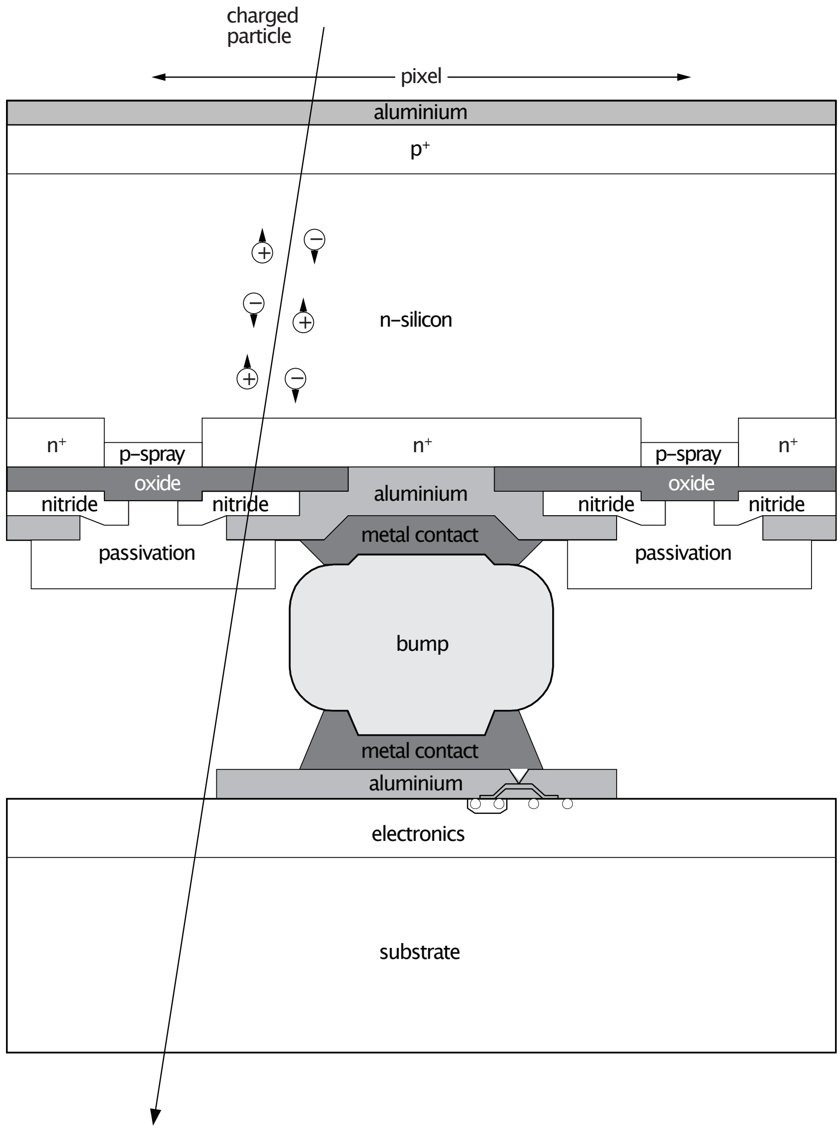

Figure 4.2: Cross-section of single pixel on a module after sensor (top) and readout chip (bottom) have been connected using the flip-chip method. Shown is a single bump connecting sensor pixel and readout electronics. The distance between sensor and readout chip is about 20 µm.

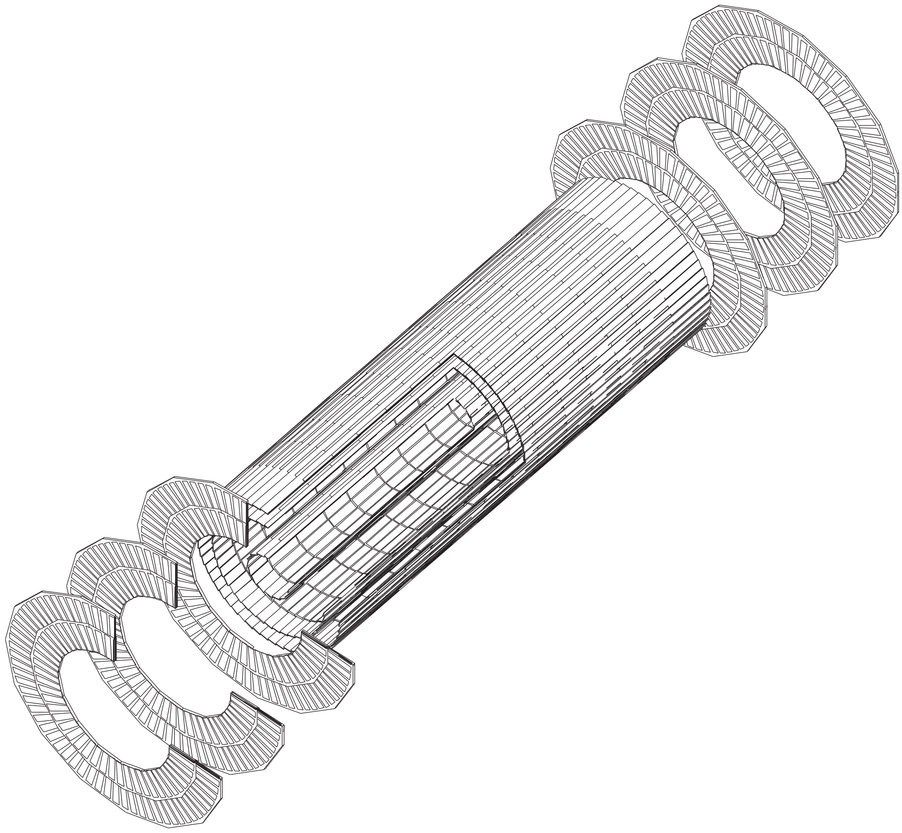

Figure 4.3: Schematic of the pixel detector with the barrel structure and end caps. The innermost B-layer is not drawn.

to the beam tube around the interaction point. The staves thus form a barrel-like structure that encloses the interaction point. Barrels with different diameters and several end-cap disks form the pixel detector. The Figure 4.3 shows the schematic design of the ATLAS pixel detector. This design achieves hermetic coverage, i.e. over a very large angular range the secondary particles generated at the interaction point pass through at least one detector layer (four measurement points per particle track for pseudorapidity[8] $|\eta| < 2.5$).

The ATLAS pixel detector has three end-caps on each side and four barrel layers. The end-caps span a radius of 88.77 mm to 149.6 mm. The three outermost barrels have radii of 122.50 mm (22 staves), 88.50 mm (38 staves), and 50.50 mm (52 staves). The innermost barrel (B-layer) has

[8]pseudorapidity is a measure of the angle θ relative to the beam axis. It is defined as $\eta = -\ln\left[\tan\left(\frac{\theta}{2}\right)\right]$. For hadron accelerators, η is used because the amount of particles per η interval is approximately constant.

a distance of 33.25 mm (14 Staves) from the proton-proton beam and has a length of 660.30 mm (14 Staves, pseudorapidity $|\eta| < 3.0$). This innermost barrel was installed in 2014 after several years of research and development to improve the efficiency of the detector at higher luminosities. An improved readout chip was developed for the new B-layer[**IBLProto**]. Compared to the FE-I3, the new FE-I4 readout chip has a larger active area with a smaller pixel size and has improved digital readout electronics optimized for higher particle track densities and particle rates.

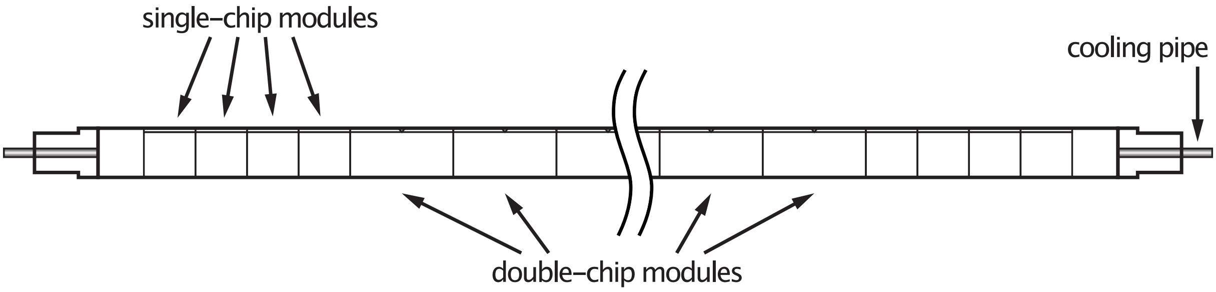

Figure 4.4: A stave of the innermost barrel (B layer). On the stave there are four FE-I4 single chip modules on each side and 12 FE-I4 double chip modules in the middle.

The stave for the B-layer contains 8 single chip modules and 12 double chip modules (a total of 32 FE-I4 readout chips, see Figure 4.4). A module consists of a sensor onto which one or two FE-I4 readout chips have been attached using the flip-chip method. A flexible printed circuit board (flex) is glued to the back of the sensor (see Figure 4.5). The flex contains traces, passive components (SMD[9]), and the connections for the supply and signal lines. The connections between the pads of the readout chip and the traces are made via wire bonds. These have a diameter of approximately 25 µm and are a few millimeters long.
In total, the pixel detector has an area of $1.7\,\mathrm{m}^2$ and consists of 1744 FE-I3 modules, which together give about 80 million readout channels (pixels). Over 12 million readout channels on 280 modules are added by the new B-layer, which has an area of about $0.15\,\mathrm{m}^2$.

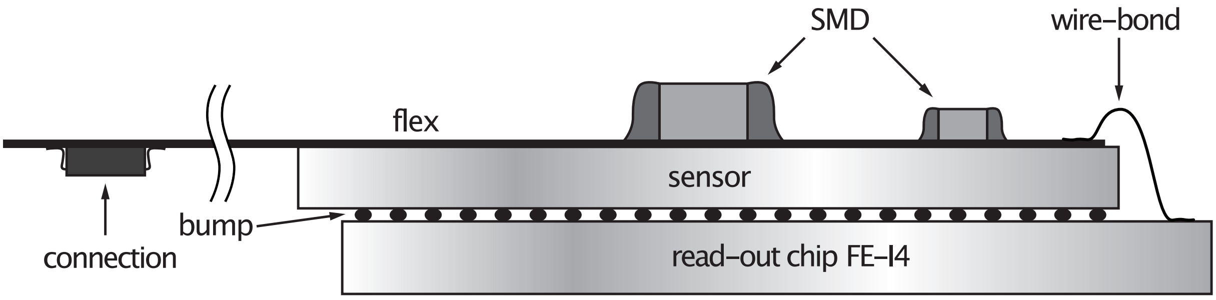

Figure 4.5: Cross-section through an FE-I4 module with flex. The module is glued to the stave with the bottom side (FE-I4). The protruding flex with the connector is only for test purposes and is cut off before mounting on the stave.

[9]**S**urface-**M**ounted **D**evice

	FE-I3	FE-I4
Technology	IBM 250 nm CMOS	IBM 130 nm CMOS
Chip size	$7.6 \times 10.8\,\text{mm}^2$	$20.2 \times 18.8\,\text{mm}^2$
Active area (matrix/total area)	74%	89%
Transistors	3,5 million	87 million
Transmission speed	40 Mb/s	160 Mb/s
Number of pixels	18×160 (2880)	80×336 (26880)
Pixel size	$50 \times 400\,\mu\text{m}^2$	$50 \times 250\,\mu\text{m}^2$
Trigger rate	100 kHz	200 kHz
Hit rate	$100\,\text{MHz/cm}^2$	$400\,\text{MHz/cm}^2$
Radiation hardness (Total Ionizing Dose)	50 Mrad	250 Mrad
Charge resolution (ToT method)	8 bit	4 bit

Table 4.1: Properties of the FE-I3 and FE-I4 readout chips.

4.2 Description of the FE-I4 readout chip

Understanding the analog electronics of the amplifier and the interaction of the individual components is relevant for this section of the experiment. The knowledge acquired in the first section of the experiment is assumed.
The FE-I4 readout chip used in this experimental section is described in more detail below. Essentially, the FE-I4 readout chip analog amplifier electronics is similar to the FE-I3. In contrast, the digital readout electronics have been greatly modified and optimized. Table 4.1 summarizes the characteristics of both readout chips.

Structure of the FE-I4 readout chip

The FE-I4 readout chip for the ATLAS pixel detector has 26880 readout channels arranged in 80 columns and 336 lines (see Figure 4.6). Each pixel has a size of $50 \times 250\,\mu\text{m}^2$ and is connected to a sensor pixel via a bump.
Each pixel of the FE-I4 readout chip consists of an analog part with **injection circuit**, **preamplifier**, **pulse shaping amplifier** and a **discriminator** and a digital part with the **readout logic** (see Figure 4.7).
The FE-I4 readout chip can be configured both globally with the global registers and locally with the pixel registers. The global registers are used to set parameters that affect the entire readout chip. These are e.g. the voltage amplitude of the injection circuit or the readout delay of the hit data. Parameters which are set with the pixel registers are e.g. output voltage of the digital-to-analog converter (DAC) for the control of the analog part or control lines for switching off single malfunctioning pixels. A local adjustment of the DACs is necessary to compensate parameter variations between the transistors of the analog part, which occur during the production of the chips.
For the operation of the FE-I4 a digital (VDDD = 1.2 V) and an analog (VDDA = 1.5 V) supply voltage is required. Furthermore, the FE-I4 requires an externally supplied system clock. The system clock has a frequency of 40 MHz corresponding to the LHC collision rate.

Figure 4.6: Photo of the FE-I4 readout chip. The pixel matrix takes up almost the entire area and is located in the upper part. The column structure is clearly visible. In total, the FE-I4 has 80 columns and 336 rows. The contact areas for the solder bumps are visible as bright dots. As a part of the digital electronics the end of column logic is located between the pixel matrix and the contact areas for the bonding wires (lower edge).

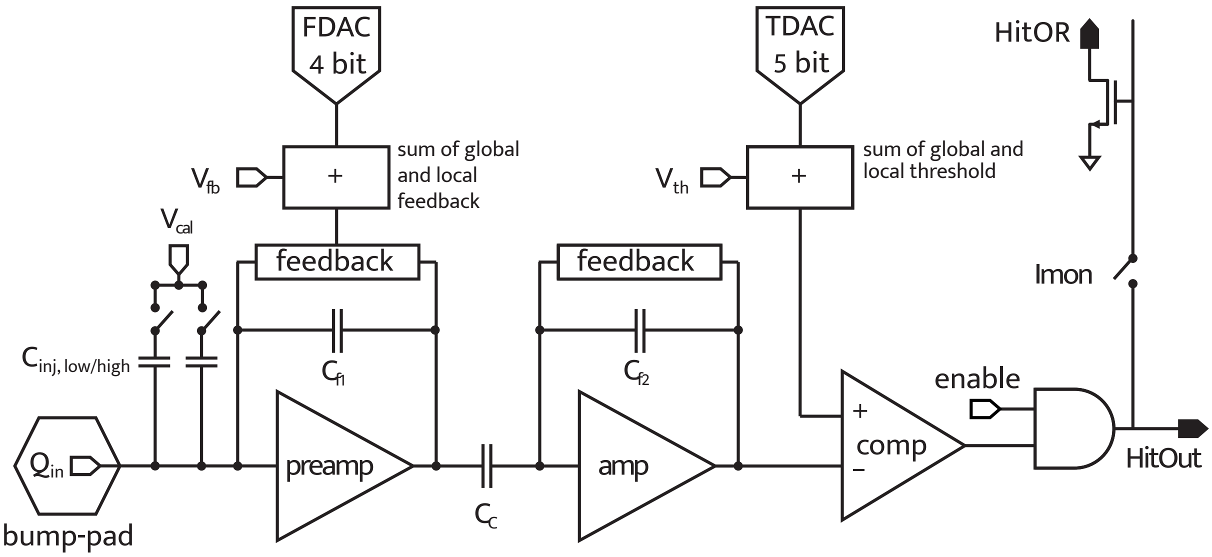

Figure 4.7: Analog circuit of a pixel. HitOut is the logical input signal for the digital circuit. The HitOut of all pixels is output via the HitOR output (logical OR). The HitOR output is accessible via a contact area on the FE-I4 readout chip.

Injection circuit

Charge can also be generated by an injection circuit instead of an ionizing particle in the sensor. The injection circuit is necessary for charge calibration and threshold measurement. As in the first part of the experiment (Charge Sensitive Amplifier in Chapter 3.2), charge can be injected into the preamplifier by a voltage step at an **injection capacitance** $\mathbf{C_{inj}}$. The charge quantity can be varied by an adjustable **voltage** $\mathbf{V_{cal}}$.
The injection capacitance size can also be varied, the adjustable sizes can be found in table 4.2. The voltage V_{cal} can be changed by the PlsrDAC register (10 bit DAC, global register).

	Design value	Measured value
$C_{\text{inj, low}}$	1.9 fF	2.0 fF ± 10%
$C_{\text{inj, high}}$	3.8 fF	4.1 fF ± 10%
$C_{\text{inj, low+high}}$	5.7 fF	6.1 fF ± 10%

Table 4.2: Design values and the average measured values of the injection capacities. Due to parameter variations, which occur during the production of the wafers, there are deviations from the design values. The measured values were obtained during module production (wafer probing) and are the average values of hundreds of readout chips.

Preamplifier and pulse shaping amplifier

An adjustable **constant current source** (feedback) discharges the **integration capacitance** C_f. The constant current source can be adjusted by the PrmpVbpf register (8 bit DAC, global register) and the FDAC register (4 bit DAC, pixel register). The preamplifier (preamp) is built in such a way that there is a nearly linear relationship between injected charge quantity and **width** of the output signal, **not the height, as in the first part of the experiment**. The preamplifier is followed by another amplifier, the pulse shaping amplifier (amp). This offers the same setting options as the preamplifier. Both amplifiers are connected by a coupling capacitance C_C to prevent possible offset DC currents. The pulse shaping amplifier amplifies the output signal of the preamplifier by the factor $C_C/C_{f2} \approx 6$.

Discriminator

The discriminator (Comp) converts the analog amplifier signal into a logic signal. The logical output signal of the discriminator (HitOut) indicates whether the voltage signal of the amplifier is above or below an adjustable **threshold**. The output has a logic one (high level) for an amplifier signal above the threshold and a logic zero (low level) for an amplifier signal below the threshold. The height of the threshold corresponds to the amount of charge at which the amplifier signal is just no longer detected as a hit. The threshold level can be set by the Vthin_AltFine register (8 bit DAC, global register) and TDAC register (5 bit DAC, pixel register). Usually the threshold is set high enough to avoid random noise hits and low enough to detect the expected charge signal.

Charge measurement

When the threshold is exceeded or undershot, time stamps are set which are temporarily stored in the digital pixel logic. The time stamps are read off a counter, which continuously increases with a supplied clock. The clock signal for the counter corresponds to the system clock of 40 MHz and is derived from the LHC collision rate.

The difference of the two time stamps is called **Time-over-Threshold** (short ToT) and corresponds to a multiple of 25 ns. Since the signal of the preamp decays linearly, the magnitude of the signal-generating charge can be obtained from the very same (see Figure 4.8). The ToT value of the hit is sent to the readout system together with the pixel address. Due to the limitation of the ToT memory to 4 bit, the charge resolution is very limited.

Detector tests and characterizations (including this part of the experiment) require a higher charge resolution. This is achieved by the **Time-to-Digital-Converter** (TDC) method using the HitOR output of the FE-I4 readout chip. All discriminator outputs are connected via a logical OR to the **HitOR** (also called Hitbus). A logical one can be read on this output terminal as soon as the amplifier signal is greater than the threshold for any pixel, and a logical zero as soon as all signals are below the threshold again. An energy spectrum can also be obtained from the HitOR signal by measuring the duration of the logic one. In the TDC method, the HitOR signal is evaluated by the readout system. The readout system uses a much higher clock rate to measure the length of the HitOR signal (640 MHz instead of 40 MHz and 12 bit resolution). The signal length is measured by a TDC implemented in the readout system.

The TDC method also has a limitation: Simultaneous hits of several pixels cannot be processed, since the measured signal length cannot be unambiguously assigned to any of the pixels. The evaluation of the measured data is constrained to cluster size[10] *one*. In addition, this measurement method requires much higher effort, because the TDC data have to be evaluated together with the hit data of the FE-I4 readout chip (ToT method).

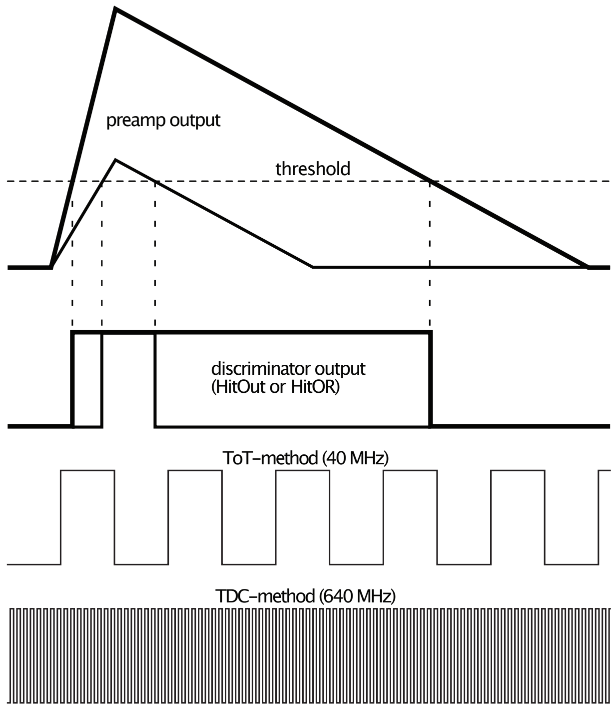

Figure 4.8: How the ToT and TDC methods work. The preamplifier signal is triangular in shape and has a rise time approximately independent of the charge quantity and a fall time adjustable by the feedback current. The length of the discriminator output signal can be measured using the ToT or TDC method.

Hit processing

If a sensor pixel is hit, the two timestamps for exceeding and falling below the threshold are temporarily stored in the pixel, as described above. After an adjustable delay time (latency), the hit data is deleted, unless a Level1 trigger occurs simultaneously with the expiration of the delay time. The Level1 trigger is a command that is sent to the FE-I4. The Level1 trigger is generated in the ATLAS detector by a complex trigger system that evaluates data from the calorimeters and the muon chambers in a very short time and can decide whether an event is interesting or not. The Level1 trigger is passed to the pixel detector readout system and from there the Level1 command is distributed to all readout chips simultaneously.

[10] The charge of a charge track of a passing particle can be distributed to several pixels, so that a hit is registered in several pixels (Shockley-Ramo theory). The measured charge of each pixel differs from the case where only a single pixel collects the complete charge. To reconstruct the original charge set, the charge values of the different pixels have to be summed up (clustering). A non-clustered charge spectrum erroneously produces a too low charge or energy distribution.

In a laboratory environment, the Level1 command can also be generated by the readout system, which also can be triggered externally. The trigger can be, for example, a scintillator signal. The FE-I4 HitOR signal can also be used as a trigger. In this case, it is called self-trigger mode.

5

Experiment II - Operation of a pixel detector

In this section the readout system required to operate a single FE-I4 readout chip is discussed. Both the hardware and software are described.

5.1 The USBpix readout system

The USBpix readout system is the hardware to which the FE-I4 readout chip is connected. The readout system is modular and the individual components are described in more detail below.

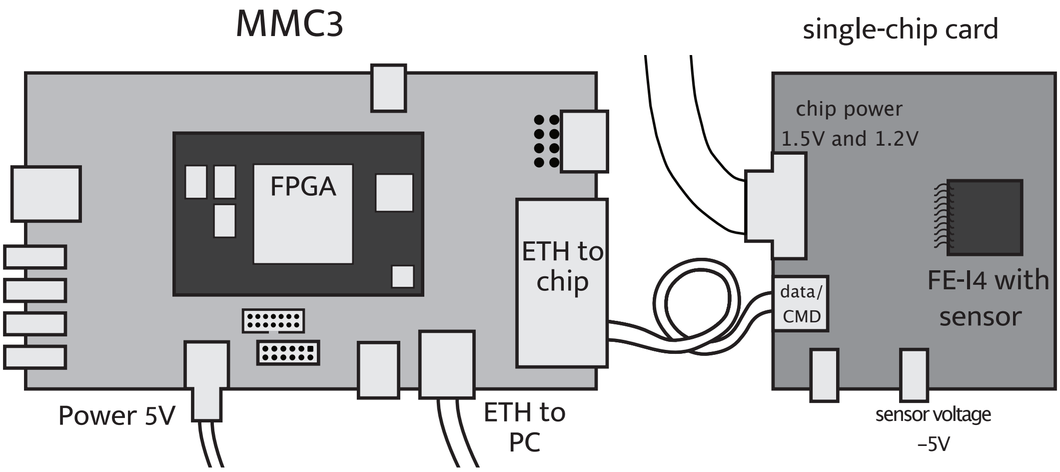

Figure 5.1: Schematic representation of the USBpix3 readout system.

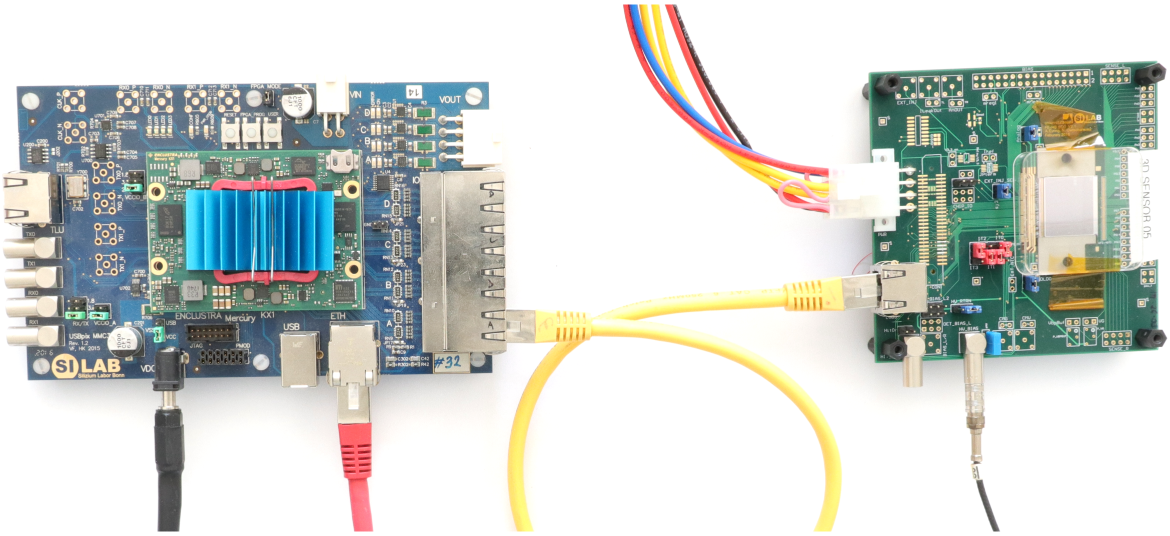

Figure 5.2: Photo of the USBpix3 readout system in operation with an FE-I4 readout chip.

MMC3 board

The Multi-chip Module Card (MMC3) was developed as part of the USBpix3 readout system to combine data transmission and power supply to and from the chip with the readout logic necessary to operate up to eight front end chips. The main part is an Kintex-7 FPGA[1] which is configured to offer the digital logic to read out the chip and create the commands as well as the SRAM for buffering chip communication. It also offers communication to the readout PC. The FPGA is provided with none volatile memory for the configuration data, so that it can self configure after a power reset. Furthermore a clock generator provides the 640 MHz FPGA and TDC clock as well as the 40 MHz FE-I4 chip clock. The front-end chips connect to the MMC3 via one of the eight sockets of the RJ-45 connector. The board is connected to the PC via ethernet and requires a supply voltage of 5 V.

Single chip card

The single-chip card enables the connection to the readout chip, meaning its contact pads. The module is glued onto the card and wire-bonds establish an electrical connection between signal lines on the card and the contact pads of the chip.
Some outputs available on the readout chip are reserved for the measurement of chip parameters, calibration and test signals. These outputs are also connected to the single-chip card and the signals can be probed via LEMO sockets or pin connectors. These are, among others, the V_{cal} voltage or the HitOR signal.
The depletion voltage for the sensor can be applied via another LEMO socket. The depletion voltage of -5 V is provided by an external SMU[2].

[1]**F**ield **P**rogrammable **G**ate **A**rray
[2]**S**ource **M**easurement **U**nit

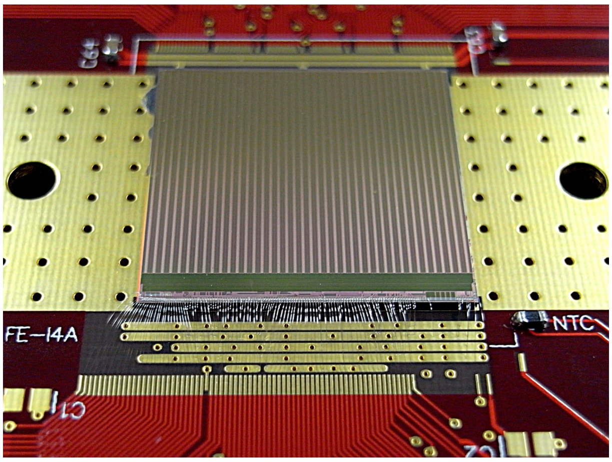

Figure 5.3: An FE-I4 readout chip without sensor on a single-chip card. The wire-bonds can be seen in the foreground.

5.2 PyBAR readout software

PyBAR[3] is the readout software used to operate the USBpix readout system and the FE-I4 readout chip. The software is written in Python and can be operated completely via the system command line (shell or terminal) or interactively with a Python interpreter. For a short introduction to Python and the IPython interpreter see Appendix 6.1.

Basics

The scripts for the individual measurements required for this part of the experiment are provided by the pyBAR readout software. No adjustments to the software or profound programming knowledge are required.
The operation of the software or the program flow (input of the commands) is given in the following Chapter 5.3. Here only general information about the operation of pyBAR is given.
PyBAR contains run scripts for various tasks. They are divided into scans, tunings and calibrations. The modules (`.py` files) have the prefix `scan_`, `tune_` and `calibrate_` respectively. Scans measure a certain state variable of the readout chip (e.g. threshold), tunings measure state variables and change the configuration of the readout chip (register values) if necessary, and calibrations measure calibration constants (e.g. V_{cal} voltage vs. PlsrDAC register).
When a run script is executed for the first time and there is no data in the output directory, the script loads the default settings into the readout chip registers (see table 5.1). A run number is generated each time a run script is executed, with the run number incremented by *one* for each run. Run numbers of successful runs can be noted to allow selection of the data obtained. A history of all runs can be found in the `run.cfg` file.
After opening the IPython interpreter by entering the command `ipython`, the following commands are necessary to execute the first run:

```
cd fei4_lab   # Directory where the software is located
```

[3] **B**onn **A**TLAS **R**eadout in Python, https://github.com/SiLab-Bonn/pyBAR

DAC	value	description
Vthin_AltFine	80	global threshold, 8 bit
TDAC	15	local threshold, 5 bit
PrmpVbpf	27	global feedback current, 8 bit
FDAC	7	local feedback current, 4 bit

Table 5.1: Extract from the default settings of the DACs. All pixel registers have the same values before the first tuning.

```
from fei4_lab import *  # Loading the necessary modules
mngr = RunManager("configuration.yaml")  # Initialization
mngr.run_run(ThresholdScan)  # Run 1 with default configuration
```

The configuration of the readout chip is also stored together with the results of the runs. These are unambiguously identifiable by the run number. The next run script loads the configuration from the previous run (Run 42 loads the configuration from Run 41 etc.). Only tuning scripts change the configuration permanently. This way it is achieved that a chain of run scripts can be executed without making special inputs for the configuration of the readout chip. In addition, when a run script is executed, any configuration can also be selected by entering a suitable parameter:

```
mngr.run_run(Fei4Tuning)  # Run 2, Changing the configuration
mngr.run_run(ThresholdScan)  # Run 3, with the configuration of Run 2 (after
    tuning)
mngr.run_run(ThresholdScan, conf={"fe_configuration": 1})  # Run 4, with the
    configuration of Run 1 (before tuning)
```

A run can be aborted at any time with [Ctrl]-[C]. Configurations from incomplete or aborted runs are not loaded, but the configuration from the last successful run is loaded.

The run scripts are briefly described below. The run scripts for this experiment are adapted to make the (measurement) results of the runs available as human-readable files (`.dat` files). Furthermore, detailed information is generated for 10 randomly selected pixels, so that all steps of the experiment can be performed for all pixels as well as for 10 individual pixels.

PlsrDacCalibration

This script measures relationship of V_{cal} vs PlsrDAC for the injection circuit. Here, the PlsrDAC is cycled from 0 to 1023 and the voltage is measured using a voltmeter connected to the readout system. The output here is a measurement curve for only one double column (here: 20, center of the readout chip).

ThresholdScan

This scan script measures the threshold and electronic noise from all pixels. By default, 100 injections are performed per PlsrDAC setting and the PlsrDAC is cycled from 0 to 100 and the

hits per pixel are counted.
For each pixel, an S-curve is created from which the threshold and electronic noise can be determined.

Fei4Tuning

This tuning script performs a complete tuning of the FE-I4 readout chip. It sets the global threshold (Vthin_AltFine) and the global feedback current (PrmpVbpf) as well as the pixel threshold (TDAC) and the pixel feedback current (FDAC).
By default, the threshold corresponds to an amount of charge equivalent to the PlsrDAC setting of 20. The feedback current is set to reach 8 ToT at a charge quantity equivalent to the PlsrDAC setting 280.

HitOrCalibration

Charge calibration of the readout chip for the ToT and TDC method. The PlsrDAC traverses a wide range of values to cover the spectrum of a radioactive source. Calibration is performed for each pixel individually to prevent overlap of the HitOR signal. 200 injections are performed per PlsrDAC setting and an average ToT and TDC value is calculated.
The charge calibration has been limited to 500 pixels to keep within the time frame.

ExtTriggerScan

Source scan in which the energy spectrum of a radioactive source is measured using the ToT and TDC methods. Here, the HitOR signal is used as a trigger signal for the readout system (self-trigger) and at the same time its length is recorded for the TDC charge measurement.
The trigger number has been limited to 100000 triggers in order to keep the time frame.
After taking the data, the measurement data are evaluated together with the charge calibrations. This is done automatically if a charge calibration has been performed before.

5.3 Experiment - Pixel detector

Make sure the sensor is fully depleted and covered to avoid leakage current induced by light.

5.3.1 Calibration of the injection circuit

By executing the scan script `PlsrDacCalibration` the calibration of the injection circuit can be done:

```
mngr.run_run(PlsrDacCalibration)
```

Task

1. Plot the V_{cal} voltage against PlsrDAC register and determine the slope and y-axis intercept. What influence can the y-axis intercept have?

Also note table 4.2 for full calibration of the injection circuit. Assume that $C_{\text{inj, low+high}}$ is used for all following steps.

5.3.2 Threshold measurement

To study the response of the system of preamplifier and discriminator, one usually considers the response function $r(Q)$:

$$r(Q) = \frac{N_{\mathrm{hit}}(Q)}{N_{\mathrm{tot}}}$$

Where N_{hit} is the number of hits in N_{tot} injections with charge Q. Ideally, one expects no hits for charge sets below a certain threshold charge $Q_{\mathrm{threshold}}$ and 100 % hit probability for charge sets above $Q_{\mathrm{threshold}}$. The response function $r(Q)$ then corresponds to a step function Θ:

$$r(Q) = \Theta(Q - Q_{\mathrm{Threshold}})$$

In the real case, the preamplifier signal has a noise component whose amplitude distribution can be assumed to be normally distributed. The noise leads to the fact that signal charges below the threshold are already recognized as hits or that signal charges above the threshold are not recognized. Then the response function is given by the convolution of the step function Θ with a Gaussian function:

$$r(Q) = \Theta(Q - Q_{\mathrm{Threshold}}) * \left(\frac{1}{\sqrt{2\pi}\sigma_{\mathrm{noise}}} e^{-Q^2/\sigma_{\mathrm{noise}}^2}\right) = \Gamma\left(\frac{Q - Q_{\mathrm{Threshold}}}{\sigma_{\mathrm{noise}}}\right)$$

$\Gamma(x)$ is the Gaussian error integral:

$$\Gamma(x) = \frac{1}{\sqrt{2\pi}} \int_0^x e^{-\frac{1}{2}t^2} \mathrm{d}t + \frac{1}{2}$$

This function is also called S-curve or error function (see Figure 5.4). Due to parameter variations

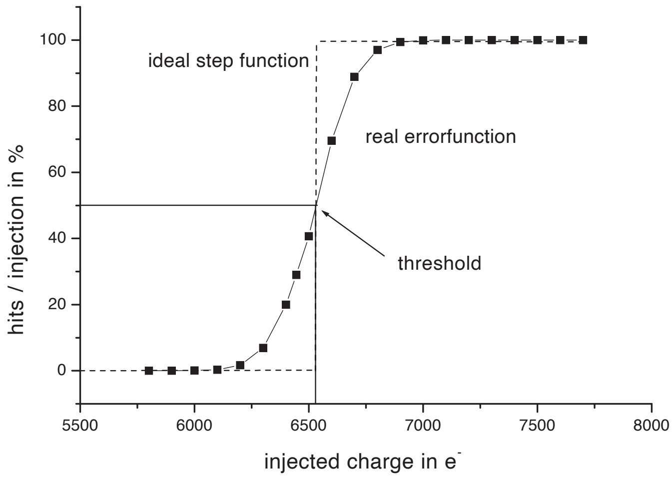

Figure 5.4: S-curve of a single pixel. The threshold (50% value) is about 6500 electrons.

of the transistors, which occur during the production of the wafers or chips, the characteristics of the transistors deviate slightly from each other. This causes the gain of the preamplifiers and the threshold of the discriminators to differ. The distribution of the thresholds of the individual pixels is a Gaussian distribution and the width $\sigma_{\text{threshold}}$ of the distribution is the threshold dispersion. By adjusting the threshold for each pixel, the threshold dispersion can be minimized. In the software, the error function is automatically fitted to the measurement data during a scan and plotted in a diagram. In the software, the PlsrDAC measurement points are placed in such a way that enough measurement points are in the range of the threshold so that the fit to the measurement data converges.

Tasks

1. Think about and explain how to graphically determine noise from an S-curve.
2. Run a threshold scan with the run script `ThresholdScan` for the entire readout chip. Determine threshold, threshold dispersion, and electronic noise for the entire readout chip. Plot the number of pixels against PlsrDAC and charge quantity (unit: number of electrons). Select a pixel and graphically determine the threshold and electronic noise. Plot the number of hits against PlsrDAC and charge quantity (unit: number of electrons).

```
mngr.run_run(ThresholdScan)
```

3. Change the global threshold (line 132 of "configuration.yaml") and run the threshold scan again.

```
mngr = RunManager("configuration.yaml") # load again the configuration
mngr.run_run(ThresholdScan)
```

4. Repeat the determination of the threshold and electronic noise for the pixel selected above.

5. Does the threshold change have an effect on the electronic noise?

6. Tune the readout chip with the run script `Fei4Tuning` and repeat the threshold scan:

```
mngr.run_run(Fei4Tuning)
threshold = mngr.current_run.register.get_global_register_value("Vthin_AltFine")
    # global threshold after tuning
threshold  # show value
mngr.run_run(ThresholdScan)
```

8. Determine threshold, threshold dispersion and electronic noise for the entire readout chip after tuning. Plot the number of pixels against PlsrDAC and charge quantity (unit: number of electrons).

9. Repeat the determination of the threshold and electronic noise for the pixel selected above.

10. What can you observe? Compare the threshold dispersion before and after tuning. Does the tuning have an effect on the electronic noise?

5.3.3 Task: Charge calibration

In this experiment, the energy spectrum of gamma radiation from a ^{241}Am source is recorded. The ToT method provides only a very low energy resolution. A higher energy resolution can be achieved with the TDC method. For both methods, a charge calibration can be performed with the run script `HitOrCalibration`:

```
mngr.run_run(HitOrCalibration)
```

1. Plot the ToT and TDC calibration for all 10 pixels on a graph, and estimate the uncertainty of charge determination of a mean ToT and TDC calibration.

2. To what ToT and TDC values does the 60 keV line of the ^{241}Am source correspond?

With the data now recorded, both an average calibration and a calibration per pixel can be performed.

5.3.4 Task : Spectroscopy of a gamma source

Record the energy spectrum of the radioactive ^{241}Am source. To do this, run the `ExtTriggerScan` run script:

```
mngr.run_run(StuckPixelScan)  # mask defective pixels
mngr.run_run(NoiseOccupancyTuning, run_conf={"occupancy_limit": 1 * 10 ** (-6)})
    # mask noisy pixels
mngr.run_run(ExtTriggerScan, run_conf={"max_triggers": 1000})  # first test with
    small number of triggers
mngr.run_run(ExtTriggerScan, run_conf={"max_triggers": 500000})  # long scan
```

The ToT value of a hit provides information about the charge deposited in the sensor (see Figure 4.8). In the ATLAS experiment this information is used to determine the position of particle tracks that produce hits in several adjacent pixels more precisely (clustering and center of gravity).

1. Compare the ToT spectrum with cluster size *one* and without clustering. Explain any possible difference. Also examine the diagram with the cluster size distribution. Do you expect a difference between gamma rays and charged particles? Why?
2. Determine the energy spectrum of the source from the ToT and TDC spectrum. Use the average ToT and TDC calibration. Compare the measured amount of charge with the expected amount of charge from the two strongest gamma lines. Can any other gamma lines be detected?
3. Compare the spectrum with medium TDC calibration and TDC calibration per pixel. Is there a difference in resolution?
4. Compare the intensities of the two strongest gamma lines. Why does the difference in event number not correspond to the intensity ratios given in the table 5.2? Use the figures 5.5 and 5.6 for your explanation and calculation. Assume that the silicon sensor has a thickness of 200 µm.

Energy (keV)	Intensity	Note
11.9	0.844 %	Ll
13.9	13.02 %	Lα
15.9	0.384 %	Lη
17.8	18.58 %	Lβ
20.8	4.83 %	Lγ
26.3	2.31 %	$\gamma_{2,1}$
33.2	0.1215 %	$\gamma_{1,0}$
43.4	0.0669 %	$\gamma_{4,2}$
59.5	35.92 %	$\gamma_{2,0}$

Table 5.2: Selected X-ray and gamma lines and intensities of an ^{241}Am source up to 60 keV. The ^{241}Am isotope decays to ^{237}Np by α-decay with a half-life of 432.6 years. There exist 5 strongly pronounced lines for this source: 3 low-energy lines between 14 keV and 21 keV due to excitation of the ^{237}Np shell, and two more lines at 26 keV and 60 keV due to nuclear transitions. Data from [**nndc**, **nucleide**].

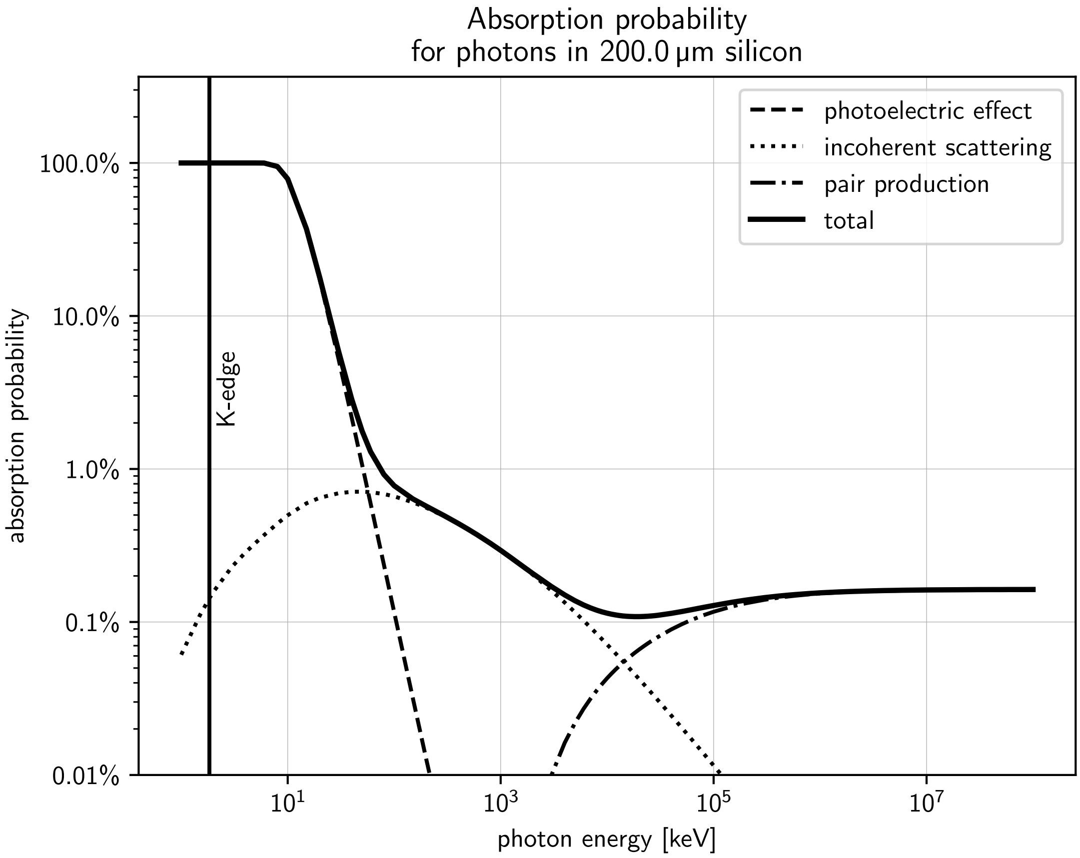

Figure 5.5: Absorption probability of photons in 200 µm silicon as a function of photon energy. Data from [**nist**].

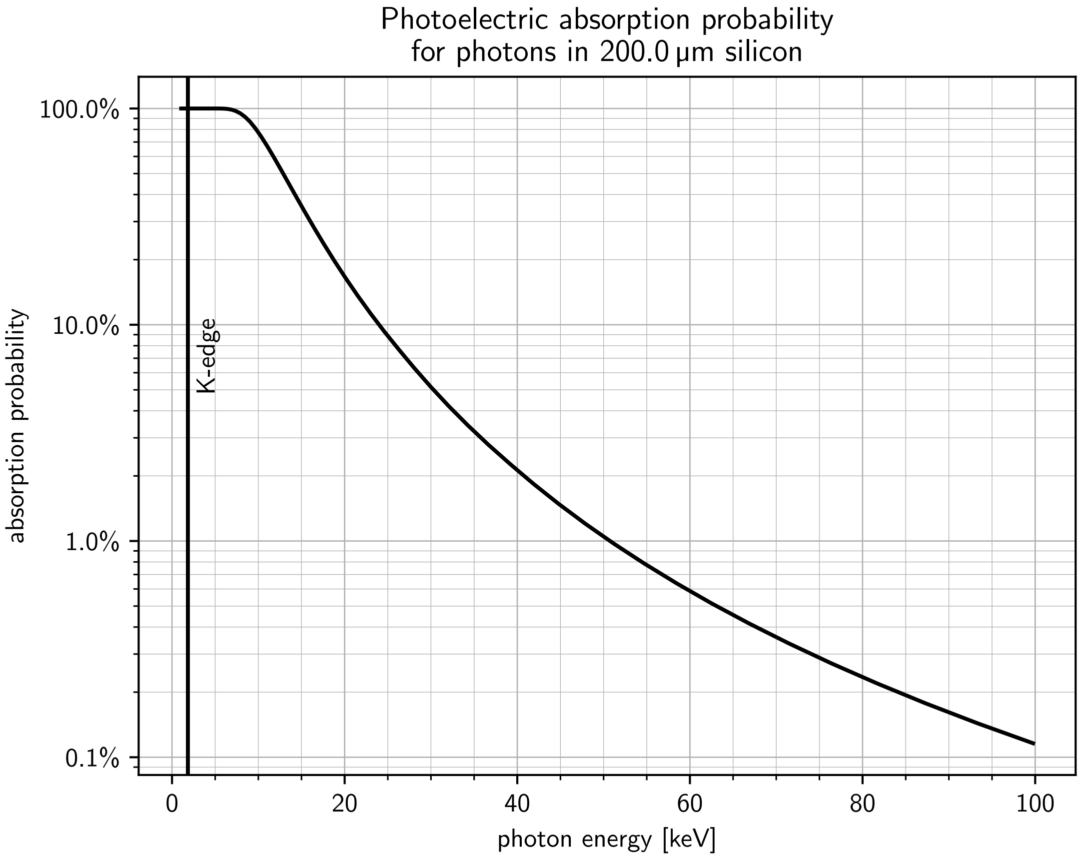

Figure 5.6: Photoelectric absorption probability of photons in 200 µm silicon. The data are based on the mass absorption coefficient of silicon. Data from [**nist2**].

6

Appendix

6.1 A short introduction to Python

In the second part of the experiment, the measurements are performed in a Python shell. Python is a scripting language, which means that the program or command does not translate into machine language until it is executed. Therefore, a Python program does not need to be compiled. In the following, a part of the syntax is described that is important for the execution of the experiment. The examples are valid for Python 2 and partially valid for Python 3.

- **Comments:** Comments start with a #.
- **Declaration of variables:** Python automatically recognizes what kind of data type[1] a value has. Variables do not have to be declared, but can be assigned a value directly:

```
a = 42             # Assignment of an integer
b = 4.2            # Floating point number
c = "hello world"  # String
```

- **Other data types:** Python knows further data types that allow a very versatile use. A distinction is made between mutable and immutable objects. An integer, floating point number and character string are immutable objects:

```
t = (1, 2, "hello")       # Tuple, immutable
t[0] = 13                 # TypeError
l = [1, 2, 3]             # List, mutable
l[2] = "hello"            # Value: [1, 2, "hello"]
f = {"Name": "Student"}   # Dictionary, mutable
f["Note"] = 3             # Value: {"Name": "Student", "Note": 3}
```

- **Calling functions:** A function `f` with parameters `x` and `y`, where `x` is to have value 27 and `y` is to have value 43, is called as follows:

[1] A data type can be, for example, an integer (int), floating point number (float), or string

```
def f(x, y):
    return x + y
f(27, 43)
f(x=27, y=43)
f(y=43, x=27)
value = f(27, y=43)
```

In the first line parameters are assigned by their position (`f` expected first `x`, then `y`). In the second and third line the parameters are specified as "keyword", the order plays little role. In the fourth line a mixture of both is used. The parameters without keyword are recognized by their position. Additionally, the return value of the function is stored in a variable. Functions can contain optional parameters, if these are not specified, a default value is used:

```
def f(x, y=43):
    return x + y
```

Functions without arguments still need parentheses:

```
def f():
    return 42
f()  # Return: 42
f    # returns function pointer
```

To call functions from a module, use the syntax

```
module.function_name(parameter)
```

- **Including modules:** Modules are, in simple terms, collections of functions, such as the lab course measurements. External modules can be included by means of the `import` command. The syntax for this is:

```
import time
time.sleep(2)  # waits 2 seconds
```

To include only one function from a module, use:

```
from time import sleep
sleep(2)  # waits 2 seconds
```

To include all functions from a module, use:

```
from time import *
sleep(2)  # waits 2 seconds
```

To include functions under a different name, use:

```
from time import sleep as wait
wait(2)  # waits 2 seconds
```

- **Output on the screen:** The `print` command:

```
a = 4
b = "hello world"
print "test", a, b  # Output: test 4 hello world
```

6.1.1 IPython

Python code can be interpreted line by line if the code is entered in a Python interpreter. Instead of the default interpreter (CPython) we use IPython (again CPython is used in the background). IPython provides some convenient features to interact with the system command line and the Python program at the same time. IPython is started from the command line by typing `ipython` and pressing <ENTER>. The following describes some functions of the interpreter that are helpful for the experiment:

- **Autocomplete:** With <TAB> commands or variable names can be expanded. Example:

```
im<TAB>
import
```

  If there is more than one possibility, it will be completed as far as it is possible and all possibilities will be issued.

```
import pos<TAB>   # show names that IPython knows
import posix      # as far as IPython can complete
```

```
posix
posixfile
posixpath
```

- **Repeat commands:** The arrow keys (▲ and ▼) can be used to select commands that have been executed previously. This is especially useful if a typo caused a program error, or if a command is to be executed more than once.

- **function return:** If a function is executed which returns a value, IPython will display it if it is not stored in a variable.

```
import time
now = time.time()   # no output, because it is stored in a variable
time.time()         # displays the return value
```

- **Help and details about the object/function/module:**

```
import time
time.time?          # short help
time.time??         # even more help
```

- **Actions on and with the command line:**

```
!ls
files = !ls
!ping uni-siegen.de
```

- **Further help:**

```
?                   # general help
%quickref           # even more help with the operation
```